HHS Public Access

Author manuscript

Exp Neurol. Author manuscript; available in PMC 2021 April 01.

Published in final edited form as:

Exp Neurol. 2020 April ; 326: 113203. doi:10.1016/j.expneurol.2020.113203.

Overexpression of Mfsd2a Attenuates Blood Brain Barrier Dysfunction via Cav-1/Keap-1/Nrf-2/HO-1 pathway in a rat model of surgical brain injury

Pinar Eser Ocak, MD[1,2], **Umut Ocak, MD**[1,3,4], **Prativa Sherchan, MBBS, PhD**[1], **Marcin Gamdzyk, PhD**[1], **Jiping Tang, MD**[1], **John H. Zhang, MD, PhD**[1,5,6,7]

[1]Department of Physiology and Pharmacology, Loma Linda University School of Medicine, Loma Linda, CA 92354, USA

[2]Department of Neurosurgery, Uludag University School of Medicine, Bursa 16120, Turkey

[3]Department of Emergency Medicine, Bursa Yuksek Ihtisas Training and Research Hospital, University of Health Sciences, Bursa 16310, Turkey

[4]Department of Emergency Medicine, Bursa City Hospital, Bursa 16110, Turkey

[5]Department of Anesthesiology, Loma Linda University School of Medicine, Loma Linda, CA 92354, USA.

[6]Department of Neurology, Loma Linda University School of Medicine, Loma Linda, CA 92354, USA.

[7]Department of Neurosurgery, Loma Linda University School of Medicine, Loma Linda, CA 92354, USA.

Abstract

Introduction: Disruption of the blood brain barrier (BBB) and subsequent cerebral edema formation is one of the major adverse effects of brain surgery, leading to postoperative neurological dysfunction. Recently, Mfsd2a has been shown to have a crucial role for the

Corresponding Author John H. Zhang, MD, PhD, Director, Center for Neuroscience Research, Professor of Anesthesiology, Neurology, Neurosurgery and Physiology, Physiology Program Director, Loma Linda University School of Medicine, Loma Linda, CA 92350, USA, Tel: 909 558-4723 Fax: 909 558-0119, johnzhang3910@yahoo.com.

Author Contributions

Literature search and hypothesis: PEO; Conception and design: PEO; Animal surgeries: PEO; Western blot experiments: PEO and UO, Neurobehavioral assessment: UO and PS; Immunohistochemical analyses: UO; Statistical analysis: PEO; Writing the manuscript: PEO; Manuscript editing: PS; Drafting the manuscript for important intellectual content: JT and JHZ; Supervision and critically revising the paper: JHZ. All authors have reviewed and approved the submitted version of the manuscript.

Ethics approval

Approval of this study was received from Institutional Animal Care and Use Committee at Loma Linda University.

Availability of data and material

The datasets generated and/or analyzed during the current study are available from the corresponding author on reasonable request.

Conflict of Interest

The authors have disclosed that they do not have any conflicts of interest.

maintenance of BBB functions. In this study, we aimed to evaluate the role of Mfsd2a on BBB disruption following surgical brain injury (SBI) in rats.

Materials and Methods: Rats were subjected to SBI by partial resection of the right frontal lobe. To evaluate the effect of Mfsd2a on BBB permeability and neurobehavior outcome following SBI, Mfsd2a was either overexpressed or downregulated in the brain by administering Mfsd2a CRISPR activation or knockout plasmids, respectively. The potential mechanism of Mfsd2a-mediated BBB protection through the cav-1/Nrf-2/HO-1 signaling pathway was evaluated.

Results: Mfsd2a levels were significantly decreased while cav-1, Nrf-2 and HO-1 levels were increased in the right frontal perisurgical area following SBI. When overexpressed, Mfsd2a attenuated brain edema and abolished neurologic impairment caused by SBI while downregulation of Mfsd2a expression further deteriorated BBB functions and worsened neurologic performance following SBI. The beneficial effect of Mfsd2a overexpression on BBB functions was associated with diminished expression of cav-1, increased Keap-1/Nrf-2 dissociation and further augmented levels of Nrf-2 and HO-1 in the right frontal perisurgical area, leading to enhanced levels of tight junction proteins following SBI. The BBB protective effect of Mfsd2a was blocked by selective inhibitors of Nrf-2 and HO-1.

Conclusions: Mfsd2a attenuates BBB disruption through cav-1/Nrf-2/HO-1 signaling pathway in rats subjected to experimental SBI.

Keywords

Blood brain barrier; brain edema; cav-1; caveolae; Mfsd2a; surgical brain injury

Introduction

Despite recent advances in microneurosurgical techniques and technologic tools used in the operation theatre to facilitate neurosurgical management of central nervous system (CNS) disorders, injury to the adjacent neural tissue due to surgery itself remains to be a challenge for neurosurgeons. Since the use of cortical incisions, suction aspirations, brain retraction systems, electrocoagulation, etc. are inevitable during majority of the brain surgeries, strategies targeting potential complications such as brain edema are mandatory (Rolston et al., 2014).

Among the major complications, disruption of the blood brain barrier (BBB) and subsequent cerebral edema formation is one of the major adverse effects of brain surgery, leading to postoperative neurological dysfunction (Rolston et al., 2014)(Wong et al., 2012)(Algattas and Huang, 2013). Unfortunately, current strategies that aim to control cerebral edema have remained unchanged for decades (Jha and Kochanek, 2018).

The development of the BBB has been shown to begin with the angiogenic phase during the development of neural tube that starts as early as E(embryonic day)9.0-E10.5 in mice. During this phase, briefly, the endothelial cells from perineural vascular plexus penetrate the neuroectoderm, giving rise to the immature brain vessels (Potente et al., 2011). During the second (differentiation, E15.5 and 18.5 in mice) phase, the newly formed vessels structure the basic BBB. Then, anti-angiogenic signals are induced and pericytes and astrocytes

recruit towards these newly formed vessels, structuring the BBB. Eventually, the third and final (maturation) phase of the BBB development is completed by the persistence and redistribution of tight junction proteins (TJP) along the whole BBB (Haddad-Tóvolli et al., 2017).

Major facilitator superfamily domain containing protein 2a (Mfsd2a) has recently been identified in the mammalian brain as the major transporter of lysophosphatidylcholine bound fatty acids, particularly docosahexaenoic acid that is an essential omega-3 fatty acid for normal brain growth and cognitive functions (PM, 2007), but not unesterified fatty acids (Nguyen et al., 2014). Moreover, it has been shown to be selectively expressed in the BBB containing microvessels of the CNS with crucial roles both in the formation and functioning of BBB (Nguyen et al., 2014)(Ben-Zvi et al., 2014). Previous studies demonstrated that the expression of Mfsd2a started at E 13.5 in the BBB that gains functionality at E15.5 (Ben-Zvi et al., 2014). Experimental studies with Mfsd2a knockout (KO) animals indicated that the absence of Mfsd2a was associated with a leaky BBB during embryogenesis as well as neonatal period and adulthood, but not with structural vascular abnormalities. These findings led researchers confirm the functional role of Mfsd2a in BBB rather than a morphogenetic role. Moreover, increased endothelial transcytosis was observed in Mfsd2a deficient animals which was associated with increased leakiness of the BBB (Ben-Zvi et al., 2014). Recent research focusing on the mechanisms of Mfsd2a-mediated regulation of BBB permeability revealed that in the absence of Mfsd2a, there was an increase in vesicular transport (transcytosis) across the endothelial cytoplasm without opening of the TJP, leading to increased BBB leakiness (Ben-Zvi et al., 2014). Interestingly, lipid transporter function of Mfsd2a was attested to be crucial in the suppression of transcytosis (Ben-Zvi et al., 2014).

Caveolin-1 (cav-1) is the major structural protein of caveolae which are flask-shaped, cholesterol rich invaginations of the plasma membrane involved in signal transduction, substrate metabolism and transcytosis. Cav-1 is essential for caveolae formation and it also governs majority of the caveolae functions (Eser Ocak et al., 2019). Importantly, increased caveolae-mediated transcytosis (CMT) has been implicated in increased BBB permeability in both rodent and human brains (Park et al., 2018)(Andreone et al., 2017)(Coelho-Santos et al., 2016).

Nuclear factor-erythroid 2–related factor-2 (Nrf-2) is a transcription factor that acts as a regulator in the antioxidant defense system and shows protective effects against endogenous and exogenous stresses (Wakabayashi et al., 2010). Under normal conditions, Nrf-2 is sequestered in the cytosol and its levels are kept low by its binder, Kelch-like ECH-associated protein-1 (Keap-1), which facilitates proteasomal degradation of Nrf-2 (Itoh et al., 2004). In case of an insult (Shah et al., 2010)(Tanaka et al., 2011), Nrf-2 is released from Keap-1, moves to the nucleus and promotes expression of cytoprotective genes such as heme oxygenase-1 (HO-1). Interestingly, previous studies have shown that knockdown of cav-1 resulted in Keap-1/Nrf-2 dissociation and subsequently increased HO-1 expression, implicating that cav-1 can inhibit Nrf-2/HO-1 complex (Li et al., 2012)(Zheng et al., 2012).

Despite current knowledge pointing to Mfsd2a as a critical player in BBB functions, its role in the regulation of BBB permeability in the setting of an insult to the brain is largely

unknown. In the present study, using a rat model of surgical brain injury (SBI), we evaluated the potential BBB protective effect of Mfsd2a following brain injury and the possible involvement of cav-1 and Keap-1/Nrf-2/HO-1 complex. Based on the above-mentioned studies, we hypothesized that overexpression of Mfsd2a may attenuate BBB disruption via cav-1/Nrf-2/HO-1 pathway following SBI in rats. Fig. 1 demonstrates the proposed mechanism for the present study.

Material and Methods

Animals and Rodent Model of Surgical Brain Injury

All experimental procedures were approved by the Institutional Animal Care and Use Committee at Loma Linda University. All procedures were in concordance with the National Institutes of Health Guide for the Care and Use of Laboratory Animals and reported according to the ARRIVE guidelines.

Adult male Sprague Dawley rats (weight 280–330 g, Envigo, IN, USA) were housed in a humidity and temperature-controlled facility for a minimum of 3 days before surgery with a 12-hour light/dark cycle and ad libitum access to food and water. Rats were randomly divided into Sham and SBI groups. The rodent model of SBI consisting of partial resection of right frontal lobe was performed (Jadhav et al., 2007b).

Briefly, rats were anesthetized with isoflurane (4% for induction, 2% for maintenance) and placed on a stereotactic frame. Under surgical microscope, midline skin incision was made, and the right frontal skull was exposed. Following a 5x5 mm right frontal craniotomy, the dura was opened, and a partial right frontal lobectomy was performed limited to the frontal area which was 1 mm anterior to the coronal suture and 2 mm lateral to the sagittal suture. Following the resection, hemostasis was obtained, and the skin was closed. Buprenorphine 0.03 mg/kg was administered subcutaneously to control postoperative pain. Sham animals underwent craniotomy only, without surgical resection of the brain tissue. Vital parameters were closely monitored and recorded during both the surgery and recovery period.

Experimental Design

Animals were randomly divided into four main experiments including time course, 24-hour outcome, 72-hour outcome and mechanism studies. The experimental design is summarized in Fig. 2. The number and distribution of animals per experimental groups are presented Table 1.

Experiment 1 (Time course study and cellular co-localization)—Endogenous expression of Mfsd2a, cav-1, Keap-1, Nrf-2, HO-1, occludin and claudin-5 was evaluated by Western blot using samples obtained from the right frontal perisurgical area (rFPA). Cellular co-localization of Mfsd2a with an endothelial cell marker (lectin) was evaluated in the right frontal perisurgical region by double-immunofluorescence staining at 24 hours following SBI.

Experiment 2 (24-hour outcome study)—In order to potentiate or downregulate the protein expression of Mfsd2a, CRISPR (**C**lustered **R**egularly **I**nterspaced **S**hort **P**alindromic

Repeat) activation (Act) or CRISPR/Cas9 KO plasmids were administered through the intracerebroventricular (icv) route. MFSD2 CRISPR/Cas9 KO plasmid (h) (Santa Cruz Biotechnology, Dallas, TX, USA; sc-405672) is a pool of 3 different gRNA plasmids including AGTCGGGCACGAACCAGATG, GGAAACAAGGCGTGTCTGCT and TCACCTGAGCCACATCCAAT whereas Mfsd2a CRISPR Act plasmid (h2) (Santa Cruz Biotechnology, Dallas, TX, USA; sc-405672-ACT) activates CTCCTAGCAATCCGAGAAGC. First, the significant alterations in Mfsd2a protein levels 24 hours after the icv injection of CRISPR Act or KO plasmids were confirmed by Western blot and reverse transcription polymerase chain reaction (RT-PCR). Next, the effect of 2 different doses of Mfsd2a CRISPR Act plasmid (2 μg and 4 μg) on neurological outcome and brain water content (BWC) was evaluated at 24 hours after SBI. The BBB protective effect of Mfsd2a overexpression was confirmed by measuring albumin extravasation using Western blot and by spectrophotometric analysis for Evans blue dye extravasation at 24 hours following SBI. Lastly, we administered Mfsd2a CRISPR KO plasmid (2 μg) through the intracerebroventricular (icv) route 24 hours prior to SBI to see whether downregulation of Mfsd2a increased BWC and deteriorated neurologic dysfunction caused by SBI.

Experiment 3 (72-hour outcome study)—The effect of Mfsd2a overexpression on neurologic outcome and BWC was evaluated at 72 hours following SBI. Based on better neurologic outcome and BWC results with Mfsd2a CRISPR Act at a dose of 2 μg during 24-hour outcome study, this dose was used for 72-hour outcome assessment.

Experiment 4 (Mechanism study)—The potential mechanism underlying protective effects of Mfsd2a overexpression on BBB integrity through cav-1/Nrf-2/HO-1 pathway was evaluated. Brusatol (Santa Cruz Biotechnology, Dallas, TX, USA; selective Nrf-2 inhibitor; 1 mg/kg) and Zinc protoporphyrin (ZnPP; Santa Cruz Biotechnology, Dallas, TX, USA; selective HO-1 inhibitor; 3 mg/kg) were used for intervention. Co-immunoprecipitation was performed to evaluate the effect of Mfsd2a overexpression on Keap-1/Nrf-2 protein interactions. Neurological outcome was evaluated at 24 hours following SBI before animals were sacrificed for sample collection.

Stereotactic Intracerebroventricular Injection and Drug Administration

Mfsd2a CRISPR Act and CRISPR/Cas9 KO plasmids and scramble (control) CRISPR products were prepared according to the manufacturer protocol. Based on previous literature evidence (Matei et al., 2018)(Okada et al., 2019)(Y. Zuo et al., 2019)(G. Zuo et al., 2019), 4 μl of the CRISPRs that were prepared according to the manufacturer's instructions were administered 24 hours before SBI through the icv route as previously described (Mo et al., 2019)(Xu et al., 2019). The time point for the administration of CRISPR products were chosen based on a previous study from our lab (Matei et al., 2018). Intracerebroventricular injection was performed under isoflurane anesthesia with the rats placed in prone position on a stereotactic frame. A burr hole was drilled at 1 mm lateral to the midline and 1.5 mm posterior to bregma. Hamilton syringe (Hamilton Co, Reno, NV) was inserted to a depth of 3.2 mm from the surface of the cortex. The drugs were injected at an injection rate of 0.5 μl/min (4 μl in total) with the aid of an infusion pump (Quintessential Stereotaxic Injector, Stoelting Co., Wood Dale, IL, USA) that is attached to the stereotactic frame. After the end

of administration of the drug, the needle was kept in position for an additional 10 minutes to prevent leakage and then withdrawn over 5 minutes. The burr hole was covered with bonewax, the skin was sutured, and the animals were allowed to recover.

Brusatol (Nrf-2 inhibitor) was diluted in 10% dimethyl sulfoxide (DMSO) and administered via icv route 30 minutes before SBI. ZnPP (HO-1 inhibitor) was diluted in 10% DMSO and administered via intravenous route 2 hours before SBI.

Assessment of Neurological Outcome

Neurobehavioral tests were performed by a blinded investigator. Modified Garcia (mGarcia) (Garcia et al., 1995), beam balance (Y. Zuo et al., 2019), and foot fault tests (Stroemer et al., 1995) were used for neurological assessment as previously described.

Modified Garcia test: Sensorimotor deficits were tested by evaluating activity in the cage, proprioception, whisker touch response, symmetry of limbs, turning, outstretching of forepaws, and climbing. The total score of the test ranged between 3 and 21 with higher scores indicating better performance in neurological testing.

Beam balance test: Motor balance and coordination were evaluated by examining ability of the animals to walk on a cylindrical beam for 60 seconds. Each animal received a score between 0 and 5 depending on the distance traveled and time to travel this distance. Higher scores indicated better performance.

Foot fault test: Locomotor function was evaluated by placing the animals on a horizontal elevated ladder. Video recording was obtained with the animals allowed to walk on the ladder for 2 minutes. The total number of steps and paw misplacements were counted for each of the limbs (Supplemental video).

Assessment of Brain Water Content

The BWC was evaluated using wet/dry method as previously described (Jadhav et al., 2007a). Briefly, the animals were sacrificed under deep anesthesia, decapitated and the brains were removed quickly. To obtain the wet weight, each sample was weighed immediately, then placed in an oven at 100°C for 48 hours and weighed again to obtain dry weights. The percentage of BWC was calculated: (wet weight – dry weight)/wet weight× 100%.

Western Blot Analysis

Western blot analysis was performed as previously described (Li et al., 2019)(Ocak et al., 2019). Briefly, after the animals were transcardially perfused with 100 mL of ice-cold chilled phosphate buffered saline (PBS, 0.01 M, pH 7.4) under deep anesthesia, the brains were removed rapidly, snap-frozen in liquid nitrogen and stored at − 80°C until use. During sample preparation, the samples obtained from rFPA were homogenized in Ripa lysis buffer (Santa Cruz Biotechnology, Dallas, TX, USA) for protein extraction and supernatants were collected after centrifugation at 14,000 g at 4 °C for 30 min. Protein concentration for each sample was determined using a detergent compatibility assay (Bio-Rad, Irvine, CA, USA).

Equal amounts of protein samples (50 μg) were separated by sodium dodecyl sulfate polyacrylamide gel electrophoresis and subsequently transferred onto nitrocellulose membranes. The membranes were blocked in blocking buffer for 1 hour at room temperature and then incubated overnight at 4 °C with the associated following primary antibodies: anti-Mfsd2a (1:500, ab105399), anti-cav-1 (1:500, ab32577), anti-Nrf-2 (1:500, ab137550), anti-HO-1 (1:500, ab13243), anti-albumin (1:1000, ab207327) (all from Abcam, Cambridge, MA, USA), anti-Keap-1 (1:500, sc-515432), anti-occludin (1:500, sc-133256) and anti-claudin-5 (1:500, sc-17668) (all from Santa Cruz Biotechnology, Dallas, TX, USA). On the following day, the membranes were incubated with the appropriate secondary antibodies (1:2000, Santa Cruz Biotechnology Inc., TX, USA) at room temperature for 1 hour. Immunoblots were visualized by ECL Plus chemiluminescence reagent kit (Amersham Bioscience, PA, USA) and quantified with optical methods using the ImageJ software (ImageJ 1.5, NIH, USA). The results were normalized using β-actin as an internal control.

Double-Immunofluorescence Staining

Double-immunofluorescence staining was performed as previously described (Mo et al., 2019). Briefly, the animals were transcardially perfused with PBS and 10% formalin under deep anesthesia. The brains were removed, post-fixed in 10% formalin at 4 °C for 24 hours and dehydrated in 30% sucrose for another 72 hours. Then the samples were embedded in OCT and sectioned into 10-μm-thick slices using a cryostat (CM3050S; Leica Microsystems, Bannockburn, IL, USA). The slices were washed in PBS (3x5 minutes) and blocked with 5% donkey serum at room temperature for 1 hour, then incubated overnight at 4 °C with the following primary antibodies: anti-Mfsd2a (1:200, ab105399), anti-lectin (1:200, ab203303) (all from Abcam, Cambridge, MA, USA). On the following day, after the sections were washed in PBS (3x5 minutes) and incubated with appropriate secondary antibodies (1:100) (Jackson Immuno Research, West Grove, PA, USA) for 1 hour at room temperature, they were visualized and photographed under a fluorescence microscope (DMi8, Leica Microsystems, Germany).

Evans Blue Dye Extravasation

The permeability of BBB was assessed using Evans blue dye extravasation assay as previously described (Uyama et al., 1988). Briefly, 5 ml/kg of 2% Evans blue dye was administered via intraperitoneal route and then allowed to circulate for 4 hours before animals were transcardially perfused with PBS and sacrificed under deep anesthesia. Brains were collected, snap-frozen in liquid nitrogen and stored at − 80°C until use. During sample preparation, brain tissues of rFPA were homogenized in PBS (1 ml/300 g) and centrifuged at 14,000 g at 4°C for 30 minutes. Supernatants were incubated overnight at 4°C with an equal amount of trichloroacetic acid (50%) and centrifuged using same parameters the next day. Extravasation of Evans blue dye was measured at 620 nm using a spectrophotometer and quantified using a standard curve and normalized to tissue weight (μg/g).

RNA isolation and quantitative RT-PCR

Total RNA was extracted using the RNeasy kit (Qiagen) and 1 μg of RNA was subjected to reverse transcription with High-Capacity cDNA Reverse Transcription Kit (Applied Biosystems, USA), following the manufacturer's instructions. Transcript levels were

measured using The QuantiTect SYBR Green PCR Kit (Qiagen) according to the manufacturer's instructions. The sequences of the primers used were as follows: Mfsd2a, Forward- 5'-CCAGGTGAAGAAGGAACCAAAA-3', Reverse- 5'-CCTCCAACCGCATAGCAAAG-3'; GAPDH, Forward- 5'-CTTCATTGACCTCAACTACATG-3', Reverse- 5'-GACTGTGCCGTTGAACTTGC-3'. Each PCR reaction mixture consisted of 50 ng of template cDNA, specific primers and QuantiTect SYBR Green PCR Master Mix for a total volume of 25 μl. The cycling program was as follows: Initial activation step-95°C for 15min, followed by 35 cycles of Denaturation- 94°C for 15s; Annealing − 55°C for 30s; Extension- 70°C for 30s and finally a melting curve analysis (60–90°C with a heating rate of 0.2 C and continuous fluorescence measurement). PCR was done in triplicate and threshold cycle numbers were averaged for each sample. Successful amplification of products was evidenced by the amplification curve and the dissociation curve. A relative fold change in expression was determined using the comparative cycle threshold method (2 –ΔΔCT).

Co-immunoprecipitation

Co-immunoprecipitation was performed according to the manufacturer's protocol using the PierceTM CoImmunoprecipitation Kit from Thermo Fisher Scientific (Grand Island, NY, USA) as previously described (Zhang et al., 2019). Briefly, the samples obtained from rFPA were lysed and extracted followed by centrifugation. After immunoprecipitation was performed using 10 μg of the anti-Nrf-2 antibody (Abcam, Cambridge, MA, USA; ab137550) by 3-hour incubation, protein G sepharose was added to the antibody-coupled resin, incubated overnight at 4 °C, and then centrifuged for 1 minute at 12000g. The resin was washed, and the protein complexes bound to the antibody were eluted. Then, the supernatant was loaded to sodium dodecyl sulfate polyacrylamide gel electrophoresis and subsequent Western blot analyses were performed as previously described to assess the protein levels of Keap-1 in the precipitates using anti-Keap-1 antibody (1: 500; Proteintech Rosemont, IL, USA; 60027-1-Ig).

Statistical Analysis

Statistical analysis was performed using GraphPad Prism 7 (GraphPad Software, San Diego, CA, USA). Quantitative data were expressed as mean ± standard deviation. One-way ANOVA followed by Tukey's post hoc test was used for comparison of different groups while Student's t-test was used to compare the independent means of 2 groups. $p<0.05$ was considered statistically significant.

Results

Mortality

A total of 204 animals were used for the present study. Of those, 165 underwent SBI while 39 underwent Sham operation. There was no mortality in the Sham group. The mortality in the SBI group was 7.9% (n=13). One animal (0.6%) was excluded from the study due to inadequate injury (Table 1).

Mfsd2a protein expression decreased after SBI

Western blot analysis of the rFPA revealed significantly decreased expression of endogenous Mfsd2a at 12, 24 and 72 hours following SBI compared to the Sham group (Fig 3A). Double-immunofluorescence staining of the rFPA demonstrated co-localization of Mfsd2a with endothelial cells in both Sham and SBI animals at 24 hours following the injury with a stronger expression in the Sham group and reduced expression after SBI compared to Sham (Fig 3B).

Expression of cav-1, Nrf-2, and HO-1 increased while occludin and claudin-5 decreased after SBI

Western blot analysis of the rFPA demonstrated increased protein levels of cav-1, which started at 12 hours and remained high up to 72 hours after SBI compared to shams. Although there was a tendency for decreased expression of Keap-1 after SBI, no statistical significance was reached. However, the expression of both Nrf-2 and HO-1 markedly increased while that of occludin and claudin-5 significantly decreased early after SBI compared to the Sham group (Fig. 3C-I).

Overexpression of Mfsd2a decreased BBB permeability and improved neurologic outcomes at 24 hours following SBI

First, by Western blot and RT-PCR analysis, we verified the protein and mRNA levels of Mfsd2a following icv administration of CRISPR. Mfsd2a protein and mRNA levels significantly increased 24 hours after the icv administration of Mfsd2a CRISPR Act plasmid (Fig. 4A, C and E). Likewise, Mfsd2a protein and mRNA levels significantly decreased 24 hours after icv administration of Mfsd2a CRISPR KO plasmid (Fig. 4B, D and E). Then, to analyze the potential BBB protective role of Mfsd2a following SBI, 2 different doses of Mfsd2a CRISPR Act plasmid (2 μg and 4 μg) were administered to overexpress Mfsd2a in the brain. The BWC in the rFPA was significantly higher in SBI groups compared to the Sham group (Fig. 5A). Both doses of Mfsd2a CRISPR Act significantly decreased brain edema and improved performance in mGarcia test (Fig. 5A, B) and decreased percentage of left and total foot faults compared to non-treated SBI groups (Fig. 5D). Beam balance score (Fig. 5C) and BWC in regions of the brain other than the rFPA showed no significant changes among groups. Although no statistical significance was reached, there was a tendency for a better treatment effect of Mfsd2a overexpression with the dose of 2 μg. Thus, based on relatively better neurologic outcomes and BWC results observed with the administration of Mfsd2a CRISPR Act at a dose of 2 μg, this dose was used for subsequent experiments.

We confirmed improved BBB functions with the overexpression of Mfsd2a by evaluating albumin leakage with Western blot and by evaluating Evans blue dye extravasation with spectrometric analysis as well. Rats subjected to SBI showed significantly increased albumin leakage and Evans blue dye extravasation in the rFPA compared to shams at 24 hours after SBI. Overexpression of Mfsd2a remarkably reduced albumin leakage and dye extravasation compared to non-treated SBI groups, further confirming the protective role of Mfsd2a on BBB functions following SBI (Fig. 6A, B).

Overexpression of Mfsd2a decreased BBB permeability and improved neurologic outcome at 72 hours following SBI

Consistent with the 24-hour outcome results, Mfsd2a overexpression significantly decreased BWC in the rFPA (Fig. 7A) and improved performance in all neurobehavior tests compared to non-treated SBI groups at 72 hours following SBI (Fig. 7B-D).

Downregulation of Mfsd2a increased BBB leakiness and deteriorated neurologic outcomes at 24 hours following SBI

Given that Mfsd2a overexpression protected the BBB, we investigated whether Mfsd2a downregulation enhanced BBB injury and worsened neurological deficits following SBI. First, with Western blot and RT-PCR analysis, we verified that the expression of Mfsd2a and mRNA levels was significantly decreased 24 hours after the icv injection of Mfsd2a CRISPR KO plasmid compared to the naive group (Fig. 4B, D and E). Assessment of BWC revealed that Mfsd2a CRISPR KO increased brain edema in the rFPA in SBI rats (Fig. 8A). Consistently, administration of Mfsd2a CRISPR KO plasmid significantly worsened performance in mGarcia and beam balance tests and increased percentage of left and total foot faults (Fig. 8B-D) compared to SBI and SBI + Scramble CRISPR KO groups at 24 hours following the injury.

Mfsd2a protected the BBB by decreasing the expression of cav-1 and Keap-1 and increasing the expression of Nrf-2 and HO-1

With the time course study, we demonstrated that SBI was associated with reduced expression of Mfsd2a and TJP. We also showed that the protein levels of cav-1, Nrf-2 and HO-1 markedly increased after SBI while Keap-1 levels did not change significantly over time (Fig. 3A-I).

Western blot analysis at 24 hours following SBI revealed that overexpression of Mfsd2a significantly reduced the expression of cav-1 and Keap-1 while further enhancing the expression of Nrf2 and HO-1 in rats subjected to SBI. Moreover, as shown in additional file 1 and Fig. 9A-H, Mfsd2a overexpression reversed the disruptive effect of SBI on TJP expression and remarkably augmented the expression of occludin and claudin-5 following SBI compared to non-treated injury groups.

Co-immunoprecipitation consistently revealed that there was no significant decrease in Keap-1/Nrf-2 binding following SBI; however, overexpression of Mfsd2a potentiated the dissociation of Nrf-2 from Keap-1 and significantly decreased Keap-1/Nrf-2 interaction at 24 hours following SBI (Fig. 10A).

Mfsd2a protected BBB through Nrf-2 and HO-1 dependent pathway

Brusatol (selective Nrf-2 inhibitor) was used to examine whether Nrf-2 was the downstream molecule in Mfsd2a-mediated BBB protection following SBI. Our results showed that Brusatol reversed the augmented expression of Nrf-2 and HO-1 in response to Mfsd2a overexpression and diminished its beneficial effect on TJP degradation, leading to decreased protein levels of occludin and claudin-5 at 24 hours after the injury compared to Mfsd2a CRISPR Act group. These results confirmed Nrf-2 as a downstream effector of Mfsd2a in

BBB protection following SBI (Supplemental Fig. 1 and Fig. 9E-H). Similarly, ZnPP (selective HO-1 inhibitor) was administered to test whether HO-1 was involved in attenuating SBI induced BBB leakiness with the overexpression of Mfsd2a. ZnPP blocked the expression of HO-1 but not Nrf-2 in Mfsd2a CRISPR Act group and reversed the beneficial effect of Mfsd2a overexpression on TJP degradation following SBI (Fig. 9F-H). These results supported the role of HO-1 in Mfsd2a-mediated BBB protection following SBI as a downstream molecule of Nrf-2. Animals in the Mfsd2a CRISPR Act group showed improved performance in mGarcia test and foot fault test which was also reversed with the administration of both Brusatol and ZnPP (Fig. 10B-D).

Discussion

Although particular interest has long been paid to avoid iatrogenic brain injury, routine neurosurgical procedures are still associated with postoperative complications that result from unavoidable brain injury inflicted by surgical maneuvers including cortical incisions, retraction injury, intraoperative hemorrhage and thermal injury due to electrocauterization that place the healthy brain tissue at the margins of the operative site at risk of injury. Unfortunately, even minimal invasive neurosurgical approaches including endoscopic procedures are associated with injury to the healthy CNS tissue to some degree, leading to particular complications (Borg et al., 2016).

How the brain reacts to this unavoidable insult has not been evaluated extensively in humans. However, data obtained from animal models has provided significant evidence regarding the pathophysiological processes involved in the surgically injured brain tissue. The rodent model of SBI based on partial resection of the right frontal lobe, which was initially defined in our lab (Jadhav et al., 2007b)(Jadhav et al., 2007a), resembles surgically induced brain injury that is encountered in humans. Evidence primarily gathered from such experimental research has consistently showed that BBB disruption is a common response of the brain tissue to surgical trauma, leading to brain edema and worse neurologic outcomes (McBride et al., 2016). The SBI rodent model is a well-established reproducible model aimed to replicate the neurosurgical damage which is induced in the rodent model by resection of a certain amount of brain tissue. The removed brain tissue in SBI model with partial right frontal lobe resection was weighted to be approximately 35 mg in previous studies from our lab and it was reported not to significantly vary between different subjects (Jadhav et al., 2007b). This type of standard resection caused injury to the surrounding brain cortex and parenchyma and produced CNS damage via neuroinflammation, neuronal death (Xiao et al., 2018), and BBB dysfunction leading to brain edema (Zakhary et al., 2020) similar to outcomes that occur during routine neurosurgical operations in clinical practice (Rolston et al., 2014)(Wong et al., 2012). Indeed, the major goal of this model was to create an injury adjacent to the resected brain area and evaluate tissue damage induced in the previously healthy perisurgical brain tissue. This model can be utilized to study molecular mechanisms and signaling pathways involved in SBI and to test potential pretreatment modalities for neuroprotection rather than mimicking a particular neurosurgical approach even though the scale of frontal lobe injury created in this model is comparable to brain tumor resection/debulking (Peker et al., 2004) and epilepsy surgery with brain tissue resection such as anterior temporal lobectomy to some degree.

The stability of the BBB is maintained through two unique properties of endothelial cells in the CNS, the presence of TJP and very low rates of transcytosis. Thus, enhanced BBB permeability in pathologic brain conditions has been attributed to either increased transcytosis (Knowland et al., 2014)(Yang et al., 2017) or increased degradation of the TJP (Zhang et al., 2019)(Yang et al., 2019). Since Mfsd2a was first identified in 2008 as a novel member of the major facilitator superfamily of membrane proteins (Angers et al., 2008), research has revealed its involvement in a number of physiological processes such as transport, cell fusion and regeneration as well as pathologic states such as inflammation, tumor formation and progression (Eser Ocak et al., 2020). Mfsd2a has recently gained attention for its critical regulatory role in the maintenance of BBB functions (Ben-Zvi et al., 2014). The protein expression of Mfsd2a has been shown to start as early as embryonic day 13.5 in the BBB in mice. In the absence of Mfsd2a, animals exhibited leaky BBB without structural abnormalities in the cerebral vasculature, supporting the functional role of Mfsd2a in BBB rather than a morphologic role. Interestingly, increased BBB permeability resulted from enhanced CMT across the endothelial cells in Mfsd2a lacking animals but not due to the opening of the TJP (Ben-Zvi et al., 2014). These findings were in line with previous reports demonstrating the association between increased CMT and leaky BBB in both the animal models (Nag, 2003) and human studies (Bell and Zlokovic, 2009), and further supported the importance of transcytosis in BBB functions (Nguyen et al., 2014). It should be noted that the previous work which revealed no structural changes in TJP in Mfsd2a deficient animals (Ben-Zvi et al., 2014) was conducted in animals that were not subjected to any prior injury to the CNS. In fact, the alterations in Mfsd2a levels in the setting of brain injury has previously been studied only in the experimental intracerebral hemorrhage model which confirmed BBB protective effect of Mfsd2a by inhibiting CMT in mice (Yang et al., 2017). Importantly, the authors showed decreased Mfsd2a levels in the injury area and also a tendency for decreased expression of TJP in Mfsd2a downregulated mice; however, no statistical difference was observed. Consistently, we found that the protein level of Mfsd2a significantly decreased in the rFPA after SBI. We therefore increased Mfsd2a expression by administering Mfsd2a CRISPR Act plasmid and evaluated whether Mfsd2a overexpression improved outcomes following SBI. Indeed, animals transiently overexpressing Mfsd2a (owing to CRISPR) had less brain edema and exhibited better neurobehavioral performance both at 24 and 72 hours following SBI. Additionally, we observed decreased Evans blue dye extravasation and less albumin leakage in animals transiently overexpressing Mfsd2a (owing to CRISPR) compared to non-treated injury groups, which confirmed the BBB protective role of Mfsd2a following SBI. Moreover, when Mfsd2a expression was downregulated prior to SBI, rats showed further increase in BWC and displayed worse performance during neurobehavior assessment compared rats with SBI alone and control groups. These results further supported the critical contribution of Mfsd2a in maintaining BBB functions after SBI. In this study, we selected CRISPR dose of 2 μg based on previous study from our group (Matei N. et al., Journal of Neuroscience, 2018). Furthermore, our Western blot and RT-PCR results showed that 2 μg of either Act or KO CRISPR can effectively alter the protein expression and mRNA levels of Mfsd2a (Fig. 4A-E). In addition, we tested another dose 4 μg to evaluate whether increasing doses may have more beneficial effects on outcomes after SBI. Since our results showed that higher dose (4 μg) was not significantly associated with further beneficial effects after SBI, we continued with the rest of experiments using 2 μg

Mfsd2a CRISPR Act. We interpret these results as 2 μg of CRISPR Act products can achieve enough enhancement in protein expression that reaches a saturation such that probably no further facilitating effects occur with higher doses. However, more preclinical in-vivo research studies are warranted on this regard.

Cav-1, the principal marker protein of caveolae, is essential for CMT such that in the absence of cav-1, caveola vesicles cannot be formed (Drab et al., 2001). Owing to this intimate relation between cav-1 and caveola, as expected, the expression of cav-1 correlates with the degree of CMT (Huang et al., 2012)(Parton, 1996). Interestingly, despite the relatively strong agreement on the role of cav-1 dependent CMT in leaky BBB following CNS injury, the results of research studies examining the role of cav-1 in TJP degradation vary greatly. For example, although increased cav-1 expression was associated with redistribution and degradation of TJP, leading to increased brain edema and worse neurologic outcomes in various studies (Nag et al., 2007)(Liu et al., 2012), some others have conversely reported its protective effect on TJP following brain injury (Choi et al., 2016). Similarly, evidence from a more recent work on ischemic brain injury emphasized that paracellular and transcellular pathways are regulated independently, even though increased cav-1 levels and CMT preceded TJP degradation in the same study (Knowland et al., 2014). Despite of the fact that the reason for inconsistent data regarding the contribution of cav-1 to TJP degradation remains largely unknown, it cannot be explained by the differences in the methodology or the experimental models conducted in the studies, as majority of them were performed in the setting of ischemic brain injury.

Mfsd2a was previously shown to attenuate CMT by its lipid transporter function (Ben-Zvi et al., 2014)(Andreone et al., 2017) which maintains the lipid composition of plasma membrane, thereby impairing the caveolae vesicle formation (Eser Ocak et al., 2020). In the present study, using rat SBI model, we demonstrated increased cav-1 expression following brain injury. Consistent with previous data, we showed that overexpression of Mfsd2a was associated with decreased cav-1 expression at 24 hours following SBI. To the best of our knowledge, we have provided the first in-vivo evidence showing decreased protein level of cav-1 in the presence of Mfsd2a, given that the alterations in cav-1 expression in response to changes in Mfsd2a protein levels has never been studied before. By this route, we have also indirectly demonstrated increased CMT following SBI, which was also effectively reduced with the overexpression of Mfsd2a.

Under resting conditions, Nrf-2 levels are kept low by its binder, Keap-1 (Itoh et al., 2004) (Kaspar et al., 2009). However, external and internal stresses stimulate the dissociation of Nrf-2 from Keap-1 and lead to increased Nrf-2 levels which promote the expression of cytoprotective genes such as HO-1 (Shah et al., 2010)(Tanaka et al., 2011)(Moreira et al., 2007). Earlier studies have demonstrated the protective effect of Nrf-2 on TJP degradation, attenuating BBB dysfunction after various types of brain injury (Zhao et al., 2007)(Kunze et al., 2015)(Janyou et al., 2017). Similarly, a number of studies showed increased expression of HO-1 following CNS injury and underlined improved BBB functions when its expression was further stimulated (Lin et al., 2007)(Shih and Yang, 2010). In several of these reports, the BBB protective effect of HO-1 through the inhibition of TJP degradation was mediated by Nrf-2 (Alfieri et al., 2013)(Yen et al., 2016). Consistently, we demonstrated that Keap-1/

Nrf-2 pathway, the key regulator of cytoprotective responses, was affected after SBI which was associated with increased levels of Nrf-2 and HO-1. However, this increase in Nrf-2 and HO-1 levels was not enough to protect the BBB against SBI, thereby leading to significantly decreased occludin and claudin-5 levels after the injury.

Recently, cells silenced for cav-1 was shown to display lower levels of Keap-1 (Petriello et al., 2014). Therefore, cav-1 was suggested to have an inhibitory effect on Nrf-2 given the increased transcriptional activity of Nrf-2 in the absence of cav-1 (Volonte et al., 2013). Consistently, we demonstrated decreased expression of Keap-1 as well as further increased expression of Nrf-2 in transiently Mfsd2a overexpressing rats (owing to CRISPR) compared to non-treated injury groups following SBI. Importantly, with co-immunoprecipitation, we showed that overexpression of Mfsd2a which led to significantly decreased cav-1 levels after SBI was associated with decreased Nrf-2 binding to Keap-1. In other words, the presence of Mfsd2a resulted in increased dissociation of Nrf-2 from its binder, which was likely a result of decreased cav-1 expression due to Mfsd2a overexpression. Additionally, Mfsd2a overexpression was associated with increased expression of occludin and claudin-5. These protective effects of Mfsd2a overexpression on TJP degradation were reversed with the selective inhibitors of Nrf-2 and HO-1, indicating Nrf-2 and HO-1 as the downstream effectors in Mfsd2a-mediated BBB protection following SBI.

Several potential limitations should be considered while interpreting the results of the present study. First, further research is needed to investigate the other potential mechanisms underlying the neuroprotective effects of inhibition of cav-1 signaling after SBI as along with transcytosis, cav-1 is involved in signal transduction and substrate metabolism (Eser Ocak et al., 2020). Similarly, detailed roles of Mfsd2a on other CNS cells, such as neurons, astrocytes, oligodendrocytes as well as microglia remains to be elucidated. Secondly, the icv route used to deliver CRISPRs may have potentially resulted in additional damage to the BBB in the CRISPR administration groups. As seen in Fig. 6, the albumin leakage and Evans blue dye extravasation in the SBI-Scramble CRISPR group seemed to be higher than SBI group, although not significantly different, which may be due to the use of icv route to deliver the drugs resulting in some BBB damage in the former group. Third, although we showed that overexpression of Mfsd2a potentiated the dissociation of Nrf-2 from Keap-1 and significantly decreased Keap-1/Nrf-2 interaction at 24 hours following SBI, we did not evaluate how overexpression of Mfsd2a is associated with decreased expression of Keap-1. Even though this can possibly be explained by decreased expression of cav-1, according to the evidence from previous reports (Petriello et al., 2014)(Volonte et al., 2013), the precise role of cav-1 on Keap-1/Nrf-2 complex is yet to be determined. Finally, although CRISPR Act products have been widely used to augment the expression of desired proteins in recent experimental research including studies from our group (Gamdzyk et al., Neuropharmacology, 2018; Matei et al., Journal of Neuroscience, 2018; Liu et al., Experimental Neurology, 2019; Zuo et al., Free Radical Biology and Medicine, 2019) there are only a few literature evidence regarding the use of CRISPR/Cas9 to achieve knockouts in adult subjects. The double stranded DNA breaks generated by CRISPR that can be used to create gene knockouts or knockins at break locations is a novel technique allowing gene editing. We elected to use CRISPR/Cas9 KO plasmid in order to downregulate the expression of Mfsd2a rather than using other ways of transient downregulation of protein

expression such as the use of short interfering RNA (siRNA) (Yang et al., 2017) that were developed to decrease gene expression. The reason behind this approach was our aim to be consistent with the type of products to be used for both augmenting and downregulating the protein expression of Mfsd2a and also to contribute to the literature regarding the use of CRISPR in neuroscience. Indeed, consistent with previous report of in-vivo use of specific CRISPR/Cas9 to knockout a particular protein expression, we observed significant decrease in the levels of our target protein, Mfsd2a (Cheng et al., 2014) but not a total knockout leading to Mfsd2a null rats. However, the level of Mfsd2a protein expression obtained in our experiments with the administration of Mfsd2a CRISPR KO was comparable with the protein levels achieved with the administration of siRNA in previous studies, (Yang et al., 2017) that allowed us to confirm further deteriorated BBB functions as well as neurobehavioral outcomes in Mfsd2a downregulated animals. Therefore, in order to avoid misunderstanding we have used the term ‘Mfsd2a downregulation’ rather than ‘Mfsd2a knockout’ throughout the paper.

Conclusions and Clinical Perspectives

Mfsd2a has recently been identified to be selectively expressed in the endothelial cells of the mammalian brain and it has been suggested as a critical player in the formation and functioning of the BBB. Its potential use as a facilitator for the drug delivery across the BBB is considered as one of the most exciting translational potentials of Mfsd2a (Eser Ocak et al., 2020). Moreover, emerging evidence including the current work point to decreased Mfsd2a levels that contribute to post-injury BBB disruption and associated neurologic dysfunction following various types of CNS injury (Yang et al., 2017). On the other hand, Mfsd2a response to particular injury types may be unique to the pathology, which are currently largely unknown and should be considered cautiously while creating specific targeted therapeutic strategies.

In the current study, we provided the first evidence of the protective role of Mfsd2a, the novel lipid transporter of the endothelial cells of the CNS, on BBB functions by preventing TJP degradation in an experimental brain injury model. This study also provides indirect evidence for decreased CMT following SBI in the presence of Mfsd2a. Based on our results, Mfsd2a-mediated BBB protection was at least partly through the cav-1/Nrf-2/HO-1 pathway. Although earlier works indicated that Mfsd2a had no effect on TJP degradation, the lack of a prior CNS injury to the subjects in those studies should be taken into account when considering the discrepancies in results from the current study (Ben-Zvi et al., 2014).

In conclusion, the results of the present study support the regulatory role of Mfsd2a on BBB permeability and suggest overexpression of Mfsd2a as a novel therapeutic target in the management of brain edema associated with neurosurgical brain trauma. Although large numbers of in vivo and in vitro studies are warranted in order to confirm the potential role of Mfsd2a in the regulation of BBB functions in the setting of CNS trauma, we believe, targeting Mfsd2a and prohibiting its loss or aiming to provide its expression at physiological levels could provide significant contributions in the management of neurologic dysfunction related to brain edema formation.

Supplementary Material

Refer to Web version on PubMed Central for supplementary material.

Acknowledgements

Funding

Funding support was provided by National Institutes of Health grant NS084921 to John H. Zhang. The funders had no role in study design, data collection or analysis, decision to publish or manuscript preparation.

List of Abbreviations

Act	Activation
BBB	Blood brain barrier
Cav-1	Caveolin-1
CMT	Caveolae-mediated transcytosis
CNS	Central nervous system
CRISPR	Clustered Regularly Interspaced Short Palindromic Repeat
DMSO	Dimethyl sulfoxide
HO-1	Heme oxygenase-1
Icv	Intracerebroventricular
Keap-1	Kelch-like ECH-associated protein-1
KO	Knockout
Mfsd2a	Major facilitator superfamily domain containing protein 2a
mGarcia	Modified Garcia
Nrf-2	Nuclear factor-erythroid 2–related factor-2
PBS	Phosphate buffered saline
rFPA	Right frontal perisurgical area
RT-PCR	Reverse transcription polymerase chain reaction
SBI	Surgical brain injury
TJP	Tight junction proteins
BWC	Brain water content
ZnPP	Zinc protoporphyrin

REFERENCES

Alfieri A, Srivastava S, Siow RCM, Cash D, Modo M, Duchen MR, Fraser PA, Williams SCR, Mann GE, 2013 Sulforaphane preconditioning of the Nrf2/HO-1 defense pathway protects the cerebral vasculature against blood-brain barrier disruption and neurological deficits in stroke. Free Radic. Biol. Med 10.1016/j.freeradbiomed.2013.08.190

Algattas H, Huang JH, 2013 Traumatic Brain Injury pathophysiology and treatments: Early, intermediate, and late phases post-injury. Int. J. Mol. Sci 10.3390/ijms15010309

Andreone BJ, Chow BW, Tata A, Lacoste B, Ben-Zvi A, Bullock K, Deik AA, Ginty DD, Clish CB, Gu C, 2017 Blood-Brain Barrier Permeability Is Regulated by Lipid Transport-Dependent Suppression of Caveolae-Mediated Transcytosis. Neuron. 10.1016/j.neuron.2017.03.043

Angers M, Uldry M, Kong D, Gimble JM, Jetten AM, 2008 Mfsd2a encodes a novel major facilitator superfamily domain-containing protein highly induced in brown adipose tissue during fasting and adaptive thermogenesis. Biochem. J 10.1042/BJ20080165

Bell RD, Zlokovic BV, 2009 Neurovascular mechanisms and blood-brain barrier disorder in Alzheimer's disease. Acta Neuropathol. 10.1007/s00401-009-0522-3

Ben-Zvi A, Lacoste B, Kur E, Andreone BJ, Mayshar Y, Yan H, Gu C, 2014 Mfsd2a is critical for the formation and function of the blood-brain barrier. Nature. 10.1038/nature13324

Borg A, Kirkman MA, Choi D, 2016 Endoscopic Endonasal Anterior Skull Base Surgery: A Systematic Review of Complications During the Past 65 Years. World Neurosurg. 10.1016/j.wneu.2015.12.105

Cheng R, Peng I, Yan Y, Cao P, Wang J, Qiu C, Tang Lichun, Liu D, Tang Li, Jin J, Huang X, He F, Zhang P, 2014 Efficient gene editing in adult mouse livers via adenoviral delivery of CRISPR/Cas9. FEBS Lett. 10.1016/j.febslet.2014.09.008

Choi KH, Kim HS, Park MS, Kim JT, Kim JH, Cho KA, Lee MC, Lee HJ, Cho KH, 2016 Regulation of Caveolin-1 Expression Determines Early Brain Edema After Experimental Focal Cerebral Ischemia. Stroke. 10.1161/STROKEAHA.116.013205

Coelho-Santos V, Socodato R, Portugal C, Leitão RA, Rito M, Barbosa M, Couraud PO, Romero IA, Weksler B, Minshall RD, Fontes-Ribeiro C, Summavielle T, Relvas JB, Silva AP, 2016 Methylphenidate-triggered ROS generation promotes caveolae-mediated transcytosis via Rac1 signaling and c-Src-dependent caveolin-1 phosphorylation in human brain endothelial cells. Cell. Mol. Life Sci 10.1007/s00018-016-2301-3

Drab M, Verkade P, Elger M, Kasper M, Lohn M, Lauterbach B, Menne J, Lindschau C, Mende F, Luft FC, Schedl A, Hailer H, Kurzchalia TV, 2001 Loss of caveolae, vascular dysfunction, and pulmonary defects in caveolin-1 gene-disrupted mice. Science (80-.). 10.1126/science.1062688

Eser Ocak P, Ocak U, Sherchan P, Zhang JH, Tang J, 2020 Insights into major facilitator superfamily domain-containing protein-2a (Mfsd2a) in physiology and pathophysiology. What do we know so far? J. Neurosci. Res. 10.1002/jnr.24327

Eser Ocak P, Ocak U, Tang J, Zhang JH, 2019 The role of caveolin-1 in tumors of the brain - functional and clinical implications. Cell. Oncol. 10.1007/s13402-019-00447-x

Gamdzyk M, Doycheva DM, Malaguit J, Enkhjargal B, Tang J, Zhang JH, 2018 Role of PPAR-β/δ/miR-17/TXNIP pathway in neuronal apoptosis after neonatal hypoxic-ischemic injury in rats. Neuropharmacology. 10.1016/j.neuropharm.2018.08.003

Garcia JH, Wagner S, Liu KF, Hu XJ, 1995 Neurological deficit and extent of neuronal necrosis attributable to middle cerebral artery occlusion in rats: Statistical validation. Stroke. 10.1161/01.str.26.4.627

Haddad-Tóvolli R, Dragano NRV, Ramalho AFS, Velloso LA, 2017 Development and function of the blood-brain barrier in the context of metabolic control. Front. Neurosci. 10.3389/fnins.2017.00224

Huang P, Zhou CM, Qin-Hu, Liu YY, Hu BH, Chang X, Zhao XR, Xu XS, Li Q, Wei XH, Mao XW, Wang CS, Fan JY, Han JY, 2012 Cerebralcare Granule® attenuates blood-brain barrier disruption after middle cerebral artery occlusion in rats. Exp. Neurol 10.1016/j.expneurol.2012.07.017

Itoh K, Tong KI, Yamamoto M, 2004 Molecular mechanism activating Nrf2-Keap1 pathway in regulation of adaptive response to electrophiles. Free Radic. Biol. Med 10.1016/j.freeradbiomed.2004.02.075

Jadhav V, Matchett G, Hsu FPK, Zhang JH, 2007a Inhibition of Src tyrosine kinase and effect on outcomes in a new in vivo model of surgically induced brain injury. J. Neurosurg 10.3171/jns.2007.106.4.680

Jadhav V, Solaroglu I, Obenaus A, Zhang JH, 2007b Neuroprotection against surgically induced brain injury. Surg. Neurol 10.1016/j.surneu.2006.07.014

Janyou A, Wicha P, Jittiwat J, Suksamrarn A, Tocharus C, Tocharus J, 2017 Dihydrocapsaicin Attenuates Blood Brain Barrier and Cerebral Damage in Focal Cerebral Ischemia/Reperfusion via Oxidative Stress and Inflammatory. Sci. Rep 10.1038/s41598-017-11181-5

Jha RM, Kochanek PM, 2018 A Precision Medicine Approach to Cerebral Edema and Intracranial Hypertension after Severe Traumatic Brain Injury: Quo Vadis? Curr. Neurol. Neurosci. Rep 10.1007/s11910-018-0912-9

Kaspar JW, Niture SK, Jaiswal AK, 2009 Nrf2:INrf2 (Keap1) signaling in oxidative stress. Free Radic. Biol. Med 10.1016/j.freeradbiomed.2009.07.035

Knowland D, Arac A, Sekiguchi KJ, Hsu M, Lutz SE, Perrino J, Steinberg GK, Barres BA, Nimmerjahn A, Agalliu D, 2014 Stepwise Recruitment of Transcellular and Paracellular Pathways Underlies Blood-Brain Barrier Breakdown in Stroke. Neuron. 10.1016/j.neuron.2014.03.003

Kunze R, Urrutia A, Hoffmann A, Liu H, Helluy X, Pham M, Reischl S, Korff T, Marti HH, 2015 Dimethyl fumarate attenuates cerebral edema formation by protecting the blood-brain barrier integrity. Exp. Neurol 10.1016/j.expneurol.2015.02.022

Li P, Zhao G, Ding Y, Wang T, Flores J, Ocak U, Wu P, Zhang T, Mo J, Zhang JH, Tang J, 2019 Rh-IFN-α attenuates neuroinflammation and improves neurological function by inhibiting NF-κB through JAK1-STAT1/TRAF3 pathway in an experimental GMH rat model. Brain. Behav. Immun 10.1016/j.bbi.2019.01.028

Li W, Liu H, Zhou J.Sen, Cao JF, Zhou XB, Choi AMK, Chen ZH, Shen HH, 2012 Caveolin-1 inhibits expression of antioxidant enzymes through direct interaction with nuclear erythroid 2 p45-related factor-2 (Nrf2). J. Biol. Chem 10.1074/jbc.M112.352336

Lin Y, Vreman HJ, Wong RJ, Tjoa T, Yamauchi T, Noble-Haeusslein LJ, 2007 Heme oxygenase-1 stabilizes the blood-spinal cord barrier and limits oxidative stress and white matter damage in the acutely injured murine spinal cord. J. Cereb. Blood Flow Metab 10.1038/sj.jcbfm.9600412

Liu J, Jin X, Liu KJ, Liu W, 2012 Matrix metalloproteinase-2-mediated occludin degradation and caveolin-1-mediated claudin-5 redistribution contribute to blood-brain barrier damage in early ischemic stroke stage. J. Neurosci 10.1523/JNEUROSCI.6409-11.2012

Liu W, Huang J, Doycheva D, Gamdzyk M, Tang J, Zhang JH, 2019 RvD1binding with FPR2 attenuates inflammation via Rac1/NOX2 pathway after neonatal hypoxic-ischemic injury in rats. Exp. Neurol 10.1016/j.expneurol.2019.112982

Matei N, Camara J, McBride D, Camara R, Xu N, Tang J, Zhang JH, 2018 Intranasal wnt3a attenuates neuronal apoptosis through Frz1/PIWIL1a/FOXM1 pathway in MCAO rats. J. Neurosci 10.1523/JNEUROSCI.2352-17.2018

McBride DW, Wang Y, Adam L, Oudin G, Louis JS, Tang J, Zhang JH, 2016 Correlation between subacute sensorimotor deficits and brain edema in rats after surgical brain injury, in: Acta Neurochirurgica, Supplementum. 10.1007/978-3-319-18497-5_55

Mo J, Enkhjargal B, Travis ZD, Zhou K, Wu P, Zhang G, Zhu Q, Zhang T, Peng J, Xu W, Ocak U, Chen Y, Tang J, Zhang J, Zhang JH, 2019 AVE 0991 attenuates oxidative stress and neuronal apoptosis via Mas/PKA/CREB/UCP-2 pathway after subarachnoid hemorrhage in rats. Redox Biol. 10.1016/j.redox.2018.09.022

Moreira TJTP, Cebere A, Cebers G, Östenson CG, Efendic S, Liljequist S, 2007 Reduced HO-1 protein expression is associated with more severe neurodegeneration after transient ischemia induced by cortical compression in diabetic Goto-Kakizaki rats. J. Cereb. Blood Flow Metab 10.1038/sj.jcbfm.9600479

Nag S, 2003 Pathophysiology of blood-brain barrier breakdown. Methods Mol. Med 10.1385/1-59259-419-0:97

Nag S, Venugopalan R, Stewart DJ, 2007 Increased caveolin-1 expression precedes decreased expression of occludin and claudin-5 during blood-brain barrier breakdown. Acta Neuropathol. 10.1007/s00401-007-0274-x

Nguyen LN, Ma D, Shui G, Wong P, Cazenave-Gassiot A, Zhang X, Wenk MR, Goh ELK, Silver DL, 2014 Mfsd2a is a transporter for the essential omega-3 fatty acid docosahexaenoic acid. Nature. 10.1038/nature13241

Ocak U, Eser Ocak P, Huang L, Zhang JH, 2019 FSLLRY-NH2 Improves Neurological Outcome After Cardiac Arrest in Rats. Turk. Neurosurg 10.5137/1019-5149.JTN.27714-19.1

Okada T, Enkhjargal B, Travis ZD, Ocak U, Tang J, Suzuki H, Zhang JH, 2019 FGF-2 Attenuates Neuronal Apoptosis via FGFR3/PI3k/Akt Signaling Pathway After Subarachnoid Hemorrhage. Mol. Neurobiol 10.1007/s12035-019-01668-9

Park MH, Lee JY, Park KH, Jung IK, Kim KT, Lee YS, Ryu HH, Jeong Y, Kang M, Schwaninger M, Gulbins E, Reichel M, Kornhuber J, Yamaguchi T, Kim HJ, Kim SH, Schuchman EH, Jin HK, Bae J. sung, 2018 Vascular and Neurogenic Rejuvenation in Aging Mice by Modulation of ASM. Neuron. 10.1016/j.neuron.2018.09.010

Parton RG, 1996 Caveolae and caveolins. Curr. Opin. Cell Biol 10.1016/S0955-0674(96)80033-0

Peker S, Abacioglu U, Sun I, Yuksel M, Pamir MN, 2004 Irradiation after surgically induced brain injury in the rat: Timing in relation to severity of radiation damage. J. Neurooncol 10.1023/B:NEON.0000040820.78643.0a

Petriello MC, Han SG, Newsome BJ, Hennig B, 2014 PCB 126 toxicity is modulated by cross-talk between caveolae and Nrf2 signaling. Toxicol. Appl. Pharmacol 10.1016/j.taap.2014.03.018

PM K, 2007 Omega-3 DHA and EPA for cognition, behavior, and mood: clinical findings and structural-functional synergies with cell membrane phospholipids. Altern. Med. Rev

Potente M, Gerhardt H, Carmeliet P, 2011 Basic and therapeutic aspects of angiogenesis. Cell. 10.1016/j.cell.2011.08.039

Rolston JD, Han SJ, Lau CY, Berger MS, Parsa AT, 2014 Frequency and predictors of complications in neurological surgery: National trends from 2006 to 2011: Clinical article. J. Neurosurg 10.3171/2013.10.JNS122419

Shah ZA, Li RC, Ahmad AS, Kensler TW, Yamamoto M, Biswal S, Doré S, 2010 The flavanol (−)-epicatechin prevents stroke damage through the Nrf2/HO1 pathway. J. Cereb. Blood Flow Metab 10.1038/jcbfm.2010.53

Shih RH, Yang CM, 2010 Induction of heme oxygenase-1 attenuates lipopolysaccharide-induced cyclooxygenase-2 expression in mouse brain endothelial cells. J. Neuroinflammation 10.1186/1742-2094-7-86

Stroemer RP, Kent TA, Hulsebosch CE, 1995 Neocortical neural sprouting, synaptogenesis, and behavioral recovery after neocortical infarction in rats. Stroke. 10.1161/01.STR.26.11.2135

Tanaka N, Ikeda Y, Ohta Y, Deguchi K, Tian F, Shang J, Matsuura T, Abe K, 2011 Expression of Keap1-Nrf2 system and antioxidative proteins in mouse brain after transient middle cerebral artery occlusion. Brain Res. 10.1016/j.brainres.2010.11.010

Uyama O, Okamura N, Yanase M, Narita M, Kawabata K, Sugita M, 1988 Quantitative evaluation of vascular permeability in the gerbil brain after transient ischemia using Evans blue fluorescence. J. Cereb. Blood Flow Metab 10.1038/jcbfm.1988.59

Volonte D, Liu Z, Musille PM, Stoppani E, Wakabayashi N, Di YP, Lisanti MP, Kensler TW, Galbiati F, 2013 Inhibition of nuclear factor-erythroid 2-related factor (Nrf2) by caveolin-1 promotes stress-induced premature senescence. Mol. Biol. Cell 10.1091/mbc.E12-09-0666

Wakabayashi N, Slocum SL, Skoko JJ, Shin S, Kensler TW, 2010 When NRF2 talks, who's listening? Antioxidants Redox Signal. 10.1089/ars.2010.3216

Wong JM, Panchmatia JR, Ziewacz JE, Bader AM, Dunn IF, Laws ER, Gawande AA, 2012 Patterns in neurosurgical adverse events: Intracranial neoplasm surgery. Neurosurg. Focus. 10.3171/2012.7.FOCUS12183

Xiao Y, Li G, Chen Y, Zuo Y, Rashid K, He T, Feng H, Zhang JH, Liu F, 2018 Milk fat globule-epidermal growth factor-8 pretreatment attenuates apoptosis and inflammation via the integrin-β3 pathway after surgical brain injury in rats. Front. Neurol 10.3389/fneur.2018.00096

Xu W, Mo J, Ocak U, Travis ZD, Enkhjargal B, Zhang T, Wu P, Peng J, Li T, Zuo Y, Shao A, Tang J, Zhang J, Zhang JH, 2019 Activation of Melanocortin 1 Receptor Attenuates Early Brain Injury in a Rat Model of Subarachnoid Hemorrhage viathe Suppression of Neuroinflammation through AMPK/TBK1/NF-κB Pathway in Rats. Neurotherapeutics. 10.1007/s13311-019-00772-x

Yang WC, Wang Q, Chi LT, Wang YZ, Cao HL, Li WZ, 2019 Therapeutic hypercapnia reduces blood-brain barrier damage possibly via protein kinase Cϵ in rats with lateral fluid percussion injury. J. Neuroinflammation 10.1186/s12974-019-1427-2

Yang YR, Xiong XY, Liu J, Wu LR, Zhong Q, Zhou K, Meng ZY, Liu L, Wang FX, Gong QW, Liao MF, Duan CM, Li J, Yang MH, Zhang Q, Gong CX, Yang QW, 2017 Mfsd2a (major facilitator superfamily domain containing 2a) attenuates intracerebral hemorrhage-induced blood-brain barrier disruption by inhibiting vesicular transcytosis. J. Am. Heart Assoc 10.1161/JAHA.117.005811

Yen TL, Chen RJ, Jayakumar T, Lu WJ, Hsieh CY, Hsu MJ, Yang CH, Chang CC, Lin YK, Lin KH, Sheu JR, 2016 Andrographolide stimulates p38 mitogen-activated protein kinase-nuclear factor erythroid-2-related factor 2-heme oxygenase 1 signaling in primary cerebral endothelial cells for definite protection against ischemic stroke in rats. Transl. Res 10.1016/j.trsl.2015.12.002

Zakhary G, Sherchan P, Li Q, Tang J, Zhang JH, 2020 Modification of kynurenine pathway via inhibition of kynurenine hydroxylase attenuates surgical brain injury complications in a male rat model. J. Neurosci. Res 10.1002/jnr.24489

Zhang T, Xu S, Wu P, Zhou K, Wu L, Xie Z, Xu W, Luo X, Li P, Ocak U, Ocak PE, Travis ZD, Tang J, Shi H, Zhang JH, 2019 Mitoquinone attenuates blood-brain barrier disruption through Nrf2/PHB2/OPA1 pathway after subarachnoid hemorrhage in rats. Exp. Neurol 10.1016/j.expneurol.2019.02.009

Zhao J, Moore AN, Redell JB, Dash PK, 2007 Enhancing expression of Nrf2-driven genes protects the blood-brain barrier after brain injury. J. Neurosci 10.1523/JNEUROSCI.1683-07.2007

Zheng Y, Morris A, Sunkara M, Layne J, Toborek M, Hennig B, 2012 Epigallocatechin-gallate stimulates NF-E2-related factor and heme oxygenase-1 via caveolin-1 displacement. J. Nutr. Biochem. 10.1016/j.jnutbio.2010.12.002

Zuo G, Zhang T, Huang L, Araujo C, Peng J, Travis Z, Okada T, Ocak U, Zhang G, Tang J, Lu X, Zhang JH, 2019 Activation of TGR5 with INT-777 attenuates oxidative stress and neuronal apoptosis via cAMP/PKCε/ALDH2 pathway after subarachnoid hemorrhage in rats. Free Radic. Biol. Med 10.1016/j.freeradbiomed.2019.09.002

Zuo Y, Huang L, Enkhjargal B, Xu W, Umut O, Travis ZD, Zhang G, Tang J, Liu F, Zhang JH, 2019 Activation of retinoid X receptor by bexarotene attenuates neuroinflammation via PPARγ/SIRT6/FoxO3a pathway after subarachnoid hemorrhage in rats. J. Neuroinflammation. 10.1186/s12974-019-1432-5

Highlights

- Mfsd2a levels decrease and contribute to the disruption of the blood brain barrier (BBB) as well as worse neurologic outcomes following surgical brain injury (SBI).
- Overexpression of Mfsd2a alleviates BBB dysfunction by decreasing tight junction degradation and improves neurologic outcomes following SBI.
- Protective effect of Mfsd2a on BBB following SBI is at least partly mediated through Cav-1/Nrf-2/HO-1 pathway.

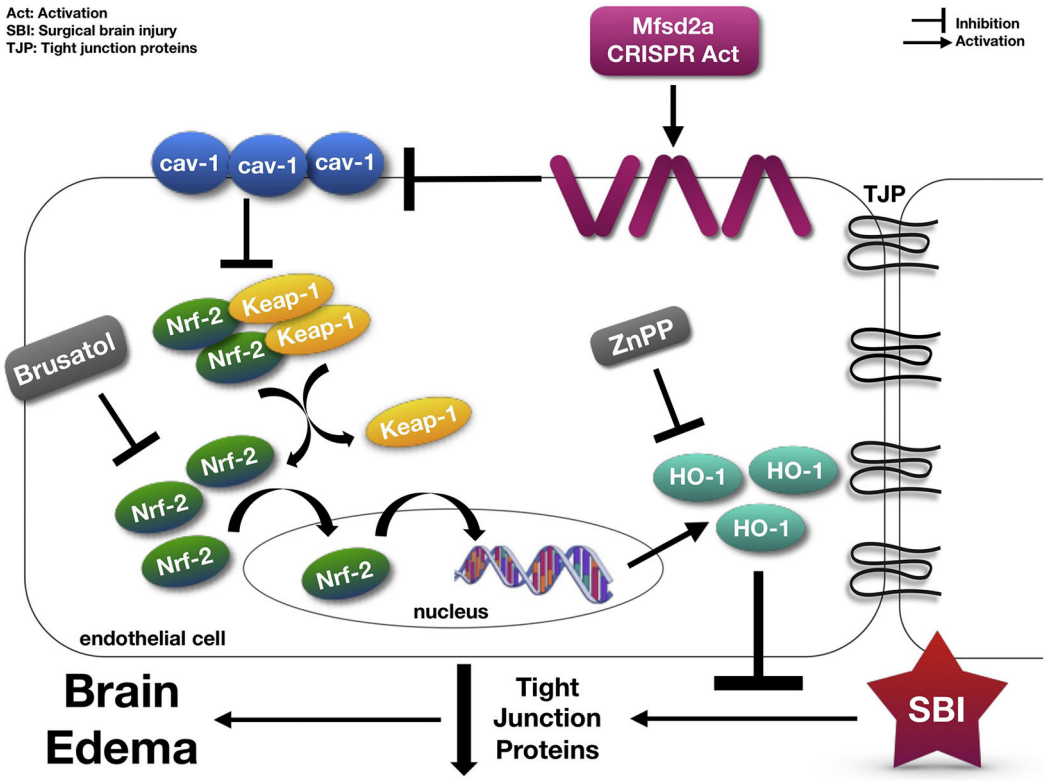

Figure 1:
The proposed mechanism for the present study.

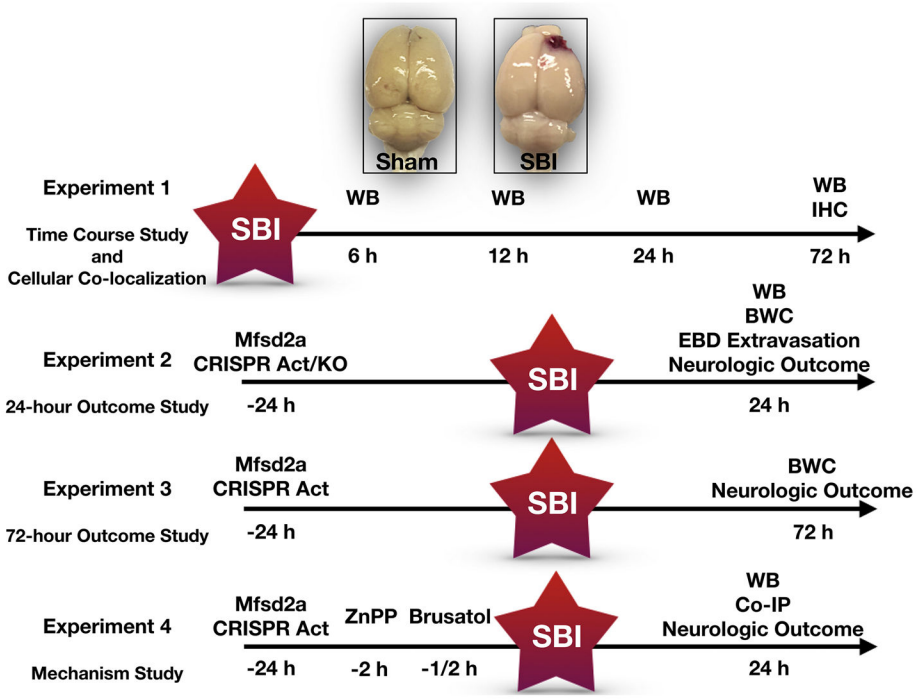

Figure 2:

Experimental design for the present study.

Act: Activation, **BWC:** Brain water content, **Co-IP:** Co-immunoprecipitation, **EBD:** Evans blue dye, **h:** hours, **IHC:** Immunohistochemistry, **KO:** Knock-out, **SBI:** Surgical brain injury, **WB:** Western blot

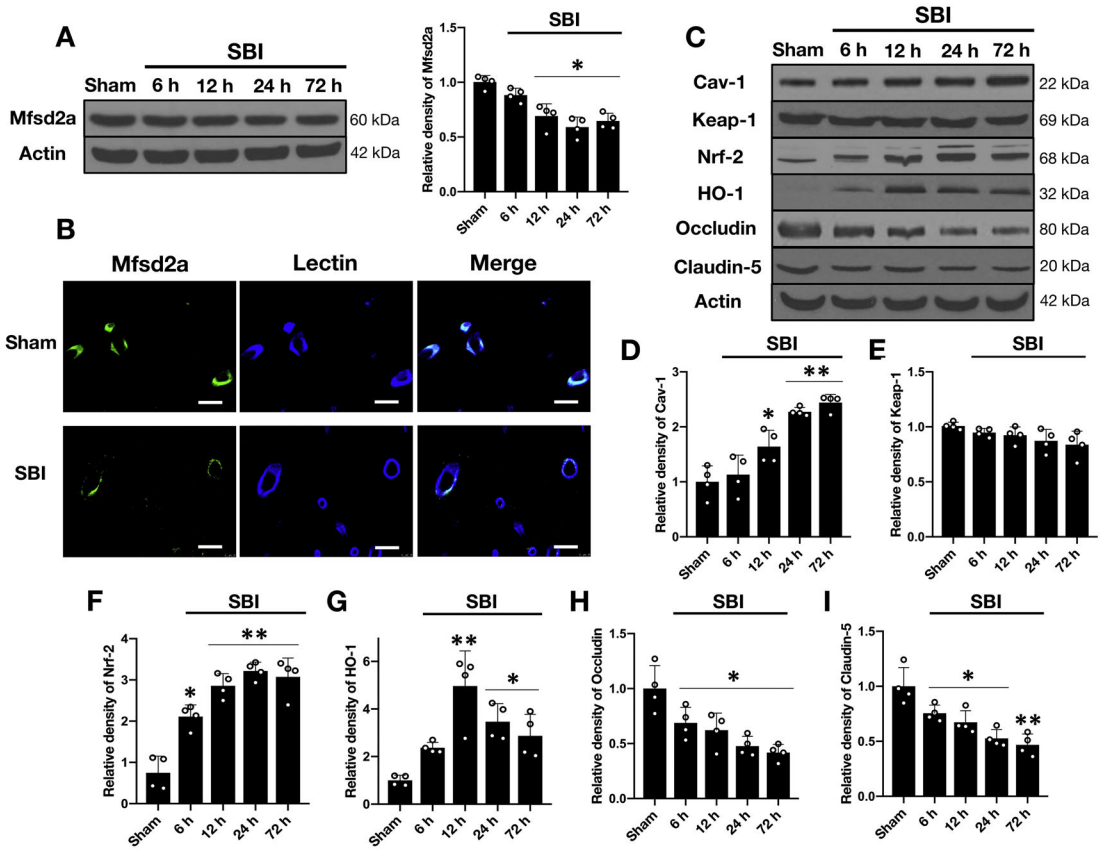

Figure 3:

Temporal expression of endogenous Mfsd2a, cav-1, Keap-1, Nrf-2, HO-1, occludin and claudin in the rFPA following SBI

A) Representative Western blot images and quantitative analyses of endogenous Mfsd2a in the rFPA revealed significantly decreased expression of Mfsd2a following SBI. Data are expressed as mean ± SD. n= 4/group. ANOVA, Tukey. *p<0.05 compared to Sham.

B) Representative immunostaining images for Mfsd2a (green) and lectin (blue) positive endothelial cells in the brain microvessels from Sham and SBI animals (rFPA) at 24 hours following the injury. The merged images of the overlay of Mfsd2a together with lectin are seen as cyan. Scale bar= 50 μm. n= 1/group.

C) Representative Western blot images and quantitative analyses of endogenous pathway proteins in the rFPA following SBI revealed increased expression of cav-1 (D), Nrf-2 (F) and HO-1 (G) while Keap-1 levels did not change significantly over 72 hours (E). The protein levels of occludin (H) and claudin-5 (I) were significantly reduced starting at 6 hours after SBI and remained low up to 72 hours. Data are expressed as mean ± SD. n= 4/group. ANOVA, Tukey. **p<0.001 compared to Sham, *p<0.05 compared to Sham.

SBI: Surgical brain injury

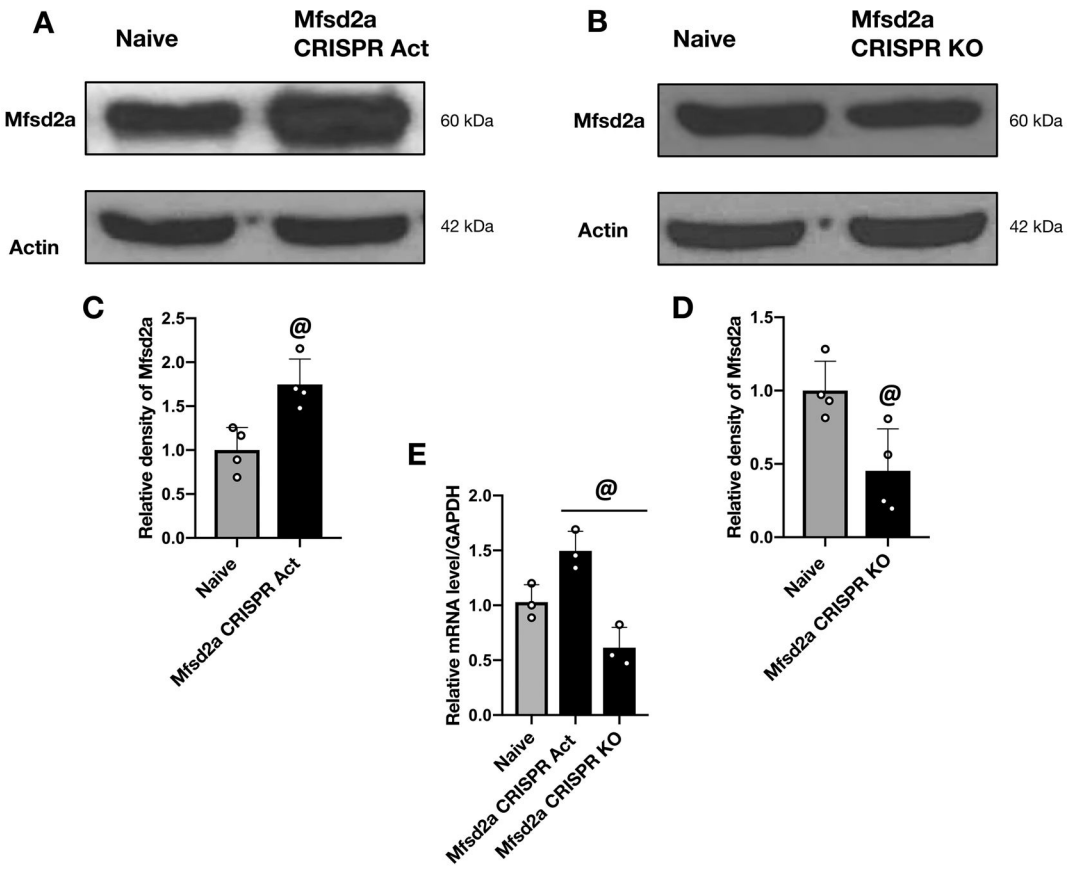

Figure 4:

Verification of alterations in Mfsd2a expression following the administration of Mfsd2a CRISPR Act and KO plasmids

Representative Western blot images and quantitative analyses of Mfsd2a protein levels in the rFPA at 24 hours following the icv administration of Mfsd2a CRISPR Act (A and C) and KO (B and D) plasmids revealed that both plasmids effectively altered Mfsd2a expression compared to naive group. RT-PCR analysis was used to confirm the alterations in mRNA levels of Mfsd2a following the administration of Mfsd2a CRISPR Act and KO plasmids compared to naive animals (E). Data are expressed as mean ± SD. n= 3/group for RT-PCR and 4/group for western blot. Student's t-test for western blot and ANOVA, Tukey for RT-PCR. @$p<0.05$ compared to naive group.

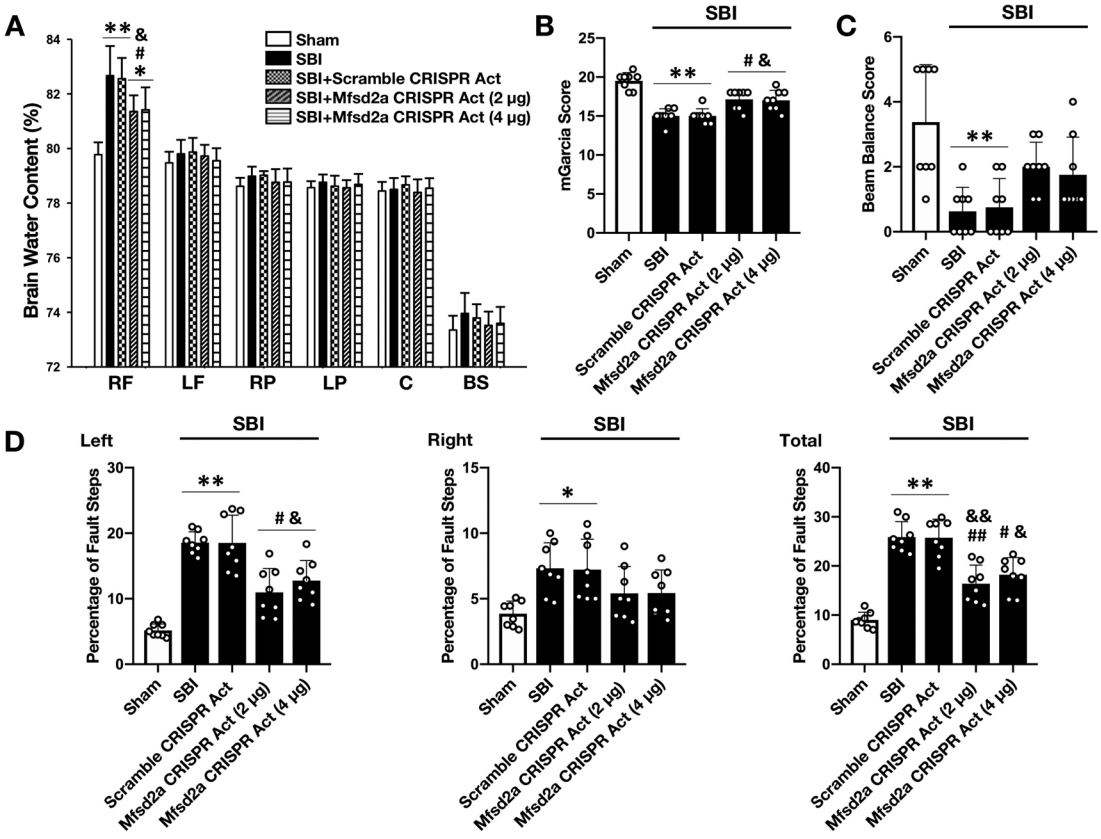

Figure 5:

Effect of Mfsd2a overexpression on BWC and neurologic outcome at 24 hours following SBI

Effect of the administration of Mfsd2a CRISPR Act plasmid on BWC (A), mGarcia score (B), beam balance score (C) and percentage of foot faults (D) at 24 hours following SBI. SBI was associated with significantly increased BWC and neurologic dysfunction in all neurologic tests compared to the Sham group at 24 hours following the injury. The administration of Mfsd2a CRISPR Act at both doses of 2 µg and 4 µg decreased brain edema and improved performance in mGarcia score and left and total foot fault counts. Data are expressed as mean ± SD. n= 8/group. ANOVA, Tukey. ** p<0.001 compared to Sham, * p<0.05 compared to Sham, ## p<0.001 compared to SBI, # p<0.05 compared to SBI, && p<0.001 compared to SBI + Scramble CRISPR Act, & p<0.05 compared to SBI + Scramble CRISPR Act.

RF: right frontal, **SBI:** Surgical brain injury, **LF:** left frontal, **RP:** right parietal, **LP:** left parietal, **C:** cerebellum, **BS:** brainstem

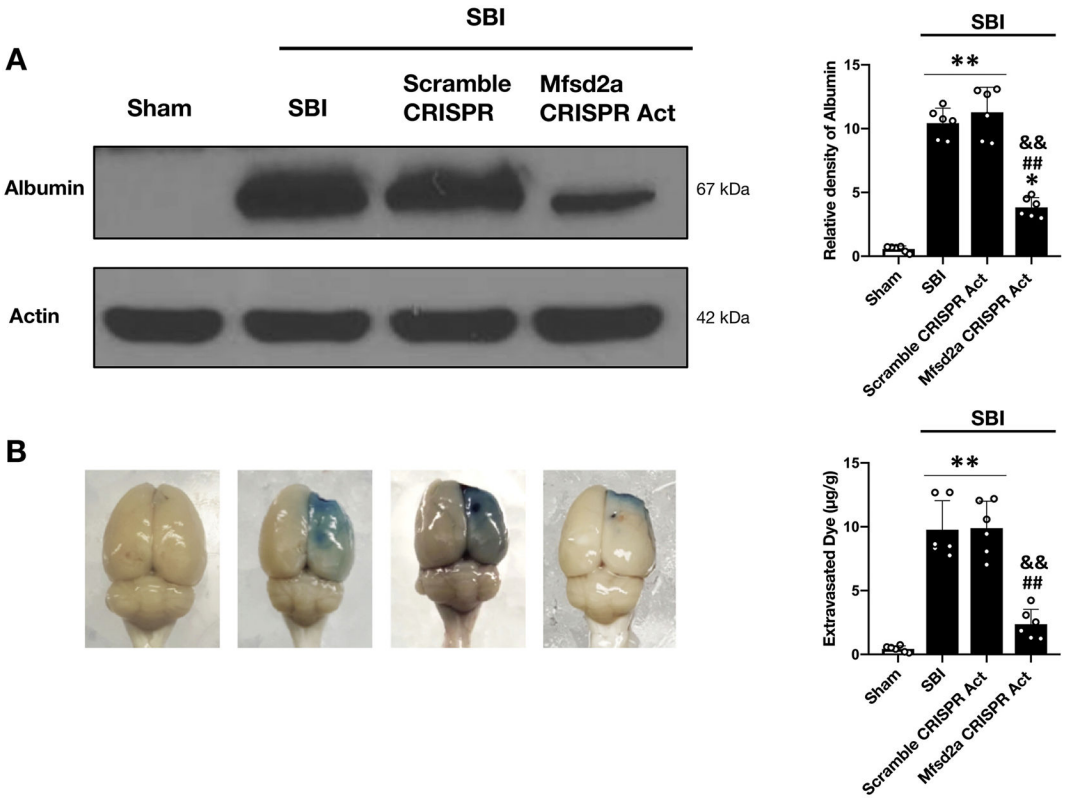

Figure 6:

Effect of Mfsd2a overexpression on albumin leakage and Evans blue dye extravasation at 24 hours following SBI

Representative images and quantitative analyses showing the degree of albumin leakage (A) and Evans blue dye extravasation (B) in the rFPA following the administration of Mfsd2a CRISPR Act plasmid (2 µg) at 24 hours after SBI. SBI was associated with increased albumin leakage and Evans blue dye extravasation compared to the Sham group. Overexpression of Mfsd2a significantly decreased albumin leakage as well as dye extravasation compared to non-treated SBI animals. Data are expressed as mean ± SD. n= 4/group for albumin leakage, n=6/group for Evans blue dye extravasation. ANOVA, Tukey. ** $p<0.001$ compared to Sham, * $p<0.05$ compared to Sham, ## $p<0.001$ compared to SBI, && $p<0.001$ compared to SBI + Scramble CRISPR Act.

SBI: Surgical brain injury

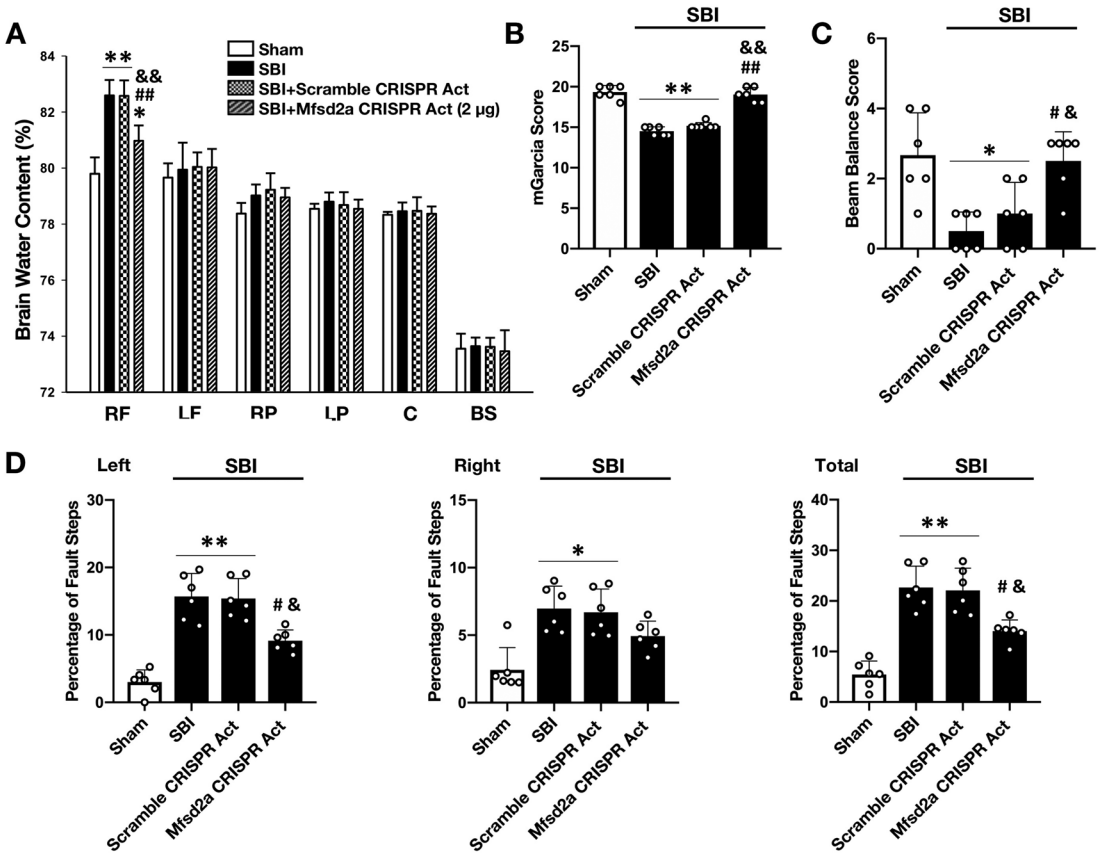

Figure 7:

Effect of Mfsd2a overexpression on BWC and neurologic outcome at 72 hours following SBI

Effect of administration of Mfsd2a CRISPR Act plasmid on BWC (A), mGarcia score (B), beam balance score (C) and percentage of foot faults (D) at 72 hours following SBI. Overexpression of Mfsd2a significantly decreased BWC and improved neurologic dysfunction caused by SBI at 72 hours after the injury. Data are expressed as mean ± SD. n= 6/group. ANOVA, Tukey. ** p<0.001 compared to Sham, * p<0.05 compared to Sham, ## p<0.001 compared to SBI, # p<0.05 compared to SBI, && p<0.001 compared to SBI + Scramble CRISPR Act, & p<0.05 compared to SBI + Scramble CRISPR Act.

RF: right frontal, **SBI:** Surgical brain injury**, LF:** left frontal, **RP:** right parietal, **LP:** left parietal, **C:** cerebellum, **BS:** brainstem

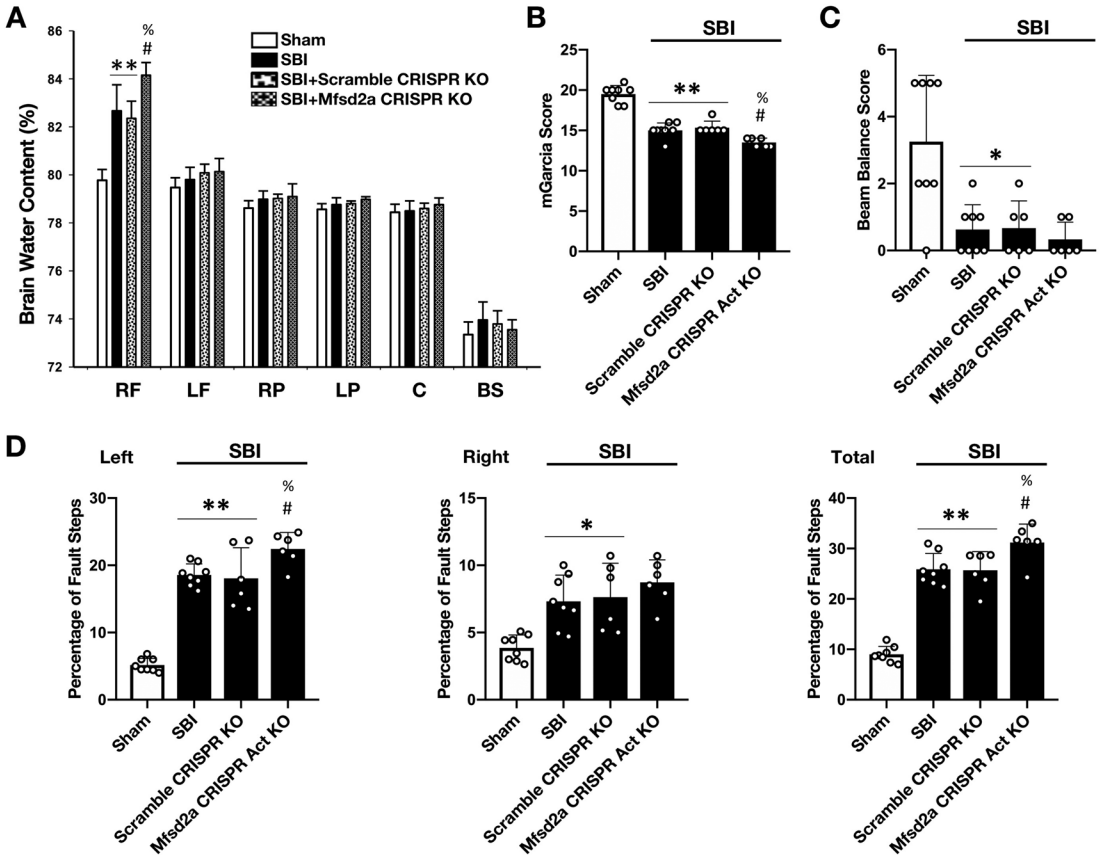

Figure 8:

Effect of Mfsd2a downregulation on BWC and neurologic outcome at 24 hours following SBI

Effect of Mfsd2a CRISPR KO plasmid on BWC (A), mGarcia score (B), beam balance score (C) and percentage of foot faults (D) at 24 hours following SBI. Downregulation of Mfsd2a was associated with further increased BWC in the rFPA compared to SBI and SBI + Scramble CRISPR KO groups. Consistently, icv administration of Mfsd2a KO plasmid worsened neurologic performance in mGarcia score, beam balance score, left and total foot fault counts. Data are expressed as mean ± SD. n= 6-8/group. ANOVA, Tukey. ** $p<0.001$ compared to Sham, * $p<0.05$ compared to Sham, # $p<0.05$ compared to SBI, % $p<0.05$ compared to SBI + Scramble CRISPR KO.

RF: right frontal, **SBI:** Surgical brain injury**, LF:** left frontal, **RP:** right parietal, **LP:** left parietal, **C:** cerebellum, **BS:** brainstem

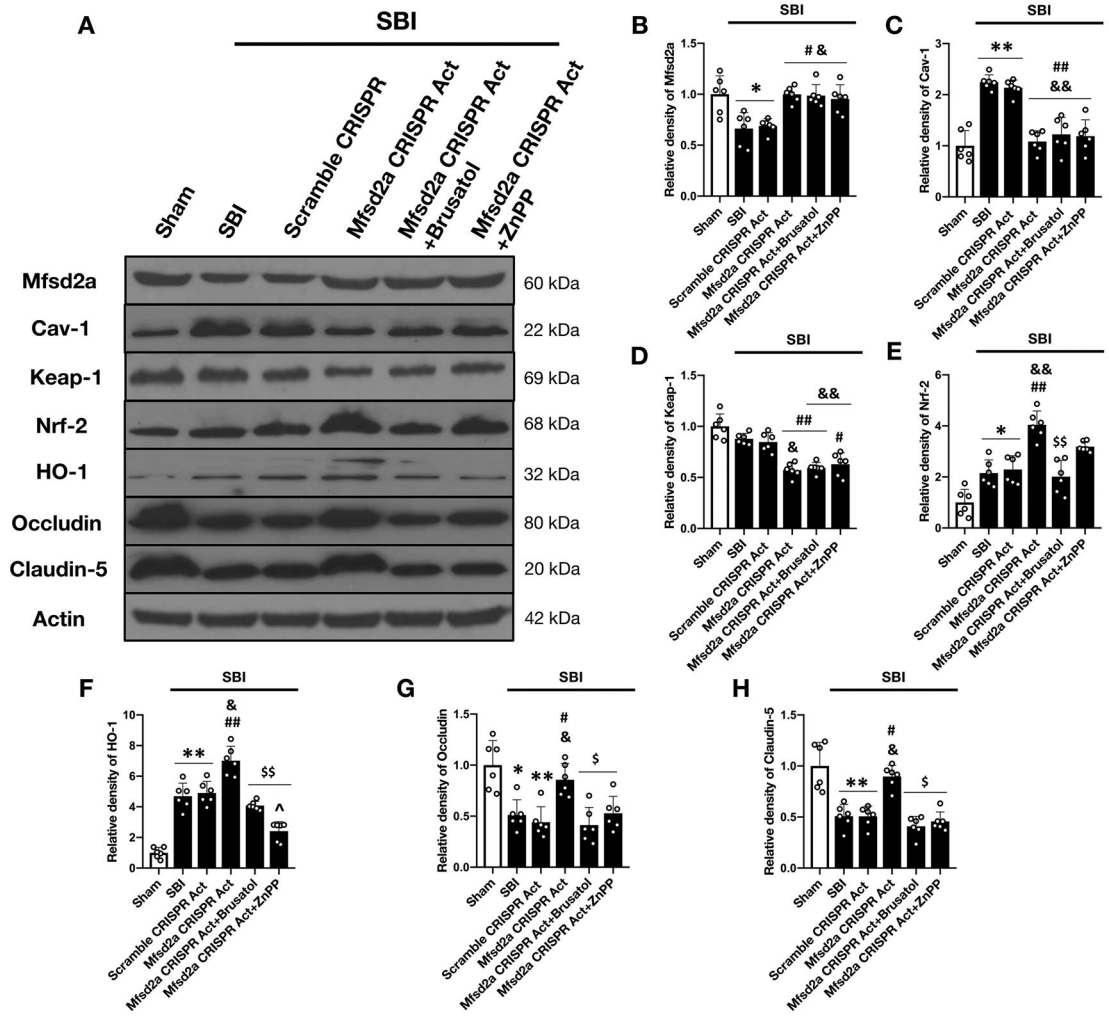

Figure 9:

Effect of Nrf-2 and HO-1 inhibition on Mfsd2a-mediated BBB protection following SBI Representative Western blot images (A) and quantitative analysis showing the expression of Mfsd2a (B), cav-1 (C), Keap-1 (D), Nrf-2 (E), HO-1 (F), occludin (G) and claudin-5 (H) at 24 hours following SBI. The overexpression of Mfsd2a was associated with significantly reduced expression of cav-1 and Keap-1 and significantly enhanced expression of Nrf2, HO-1 and TJP compared to non-treated injury groups following SBI. The administration of both Brusatol and ZnPP diminished the BBB protective effect of Mfsd2a and led to reduced expression of occludin and claudin-5 compared to Mfsd2a CRISPR Act group at 24 hours following SBI. Data are expressed as mean ± SD. n= 6/group. ANOVA, Tukey. ** $p<0.001$ compared to Sham, * $p<0.05$ compared to Sham, ## $p<0.001$ compared to SBI, # $p<0.05$ compared to SBI, && $p<0.001$ compared to SBI + Scramble CRISPR Act, & $p<0.05$ compared to SBI + Scramble CRISPR Act, $$ $p<0.001$ compared to SBI + Mfsd2a CRISPR Act (2 μg), $ $p<0.05$ compared to SBI + Mfsd2a CRISPR Act (2 μg), ^ $p<0.05$ compared to SBI + Mfsd2a CRISPR Act (2 μg) + Brusatol.

SBI: Surgical brain injury

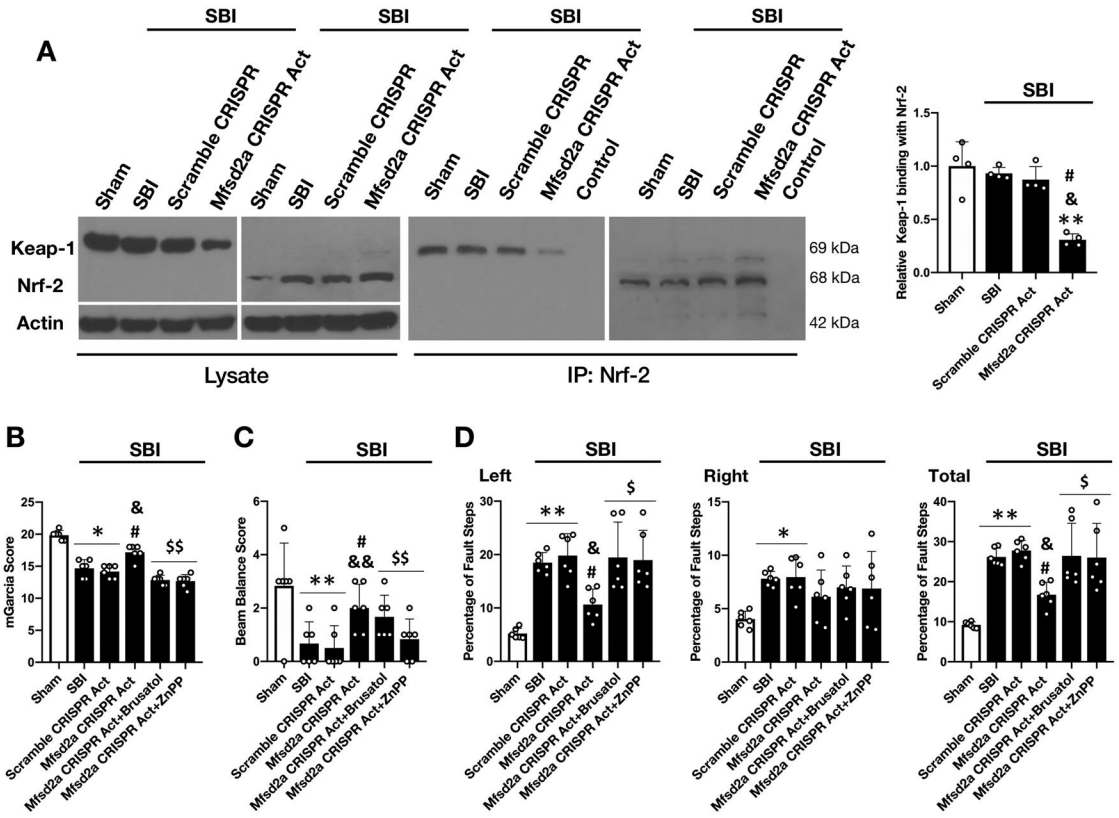

Figure 10:

Effect of Mfsd2a overexpression on Keap-1/Nrf-2 interaction and effect of Nrf-2 and HO-1 inhibition on neurologic outcome at 24 hours following SBI

A) Representative Western blot images and quantitative analysis demonstrating the effect of Mfsd2a CRISPR Act on Keap-1 co-immunoprecipitation with Nrf2 revealed that overexpression of Mfsd2a significantly increased Nrf-2 dissociation from Keap-1 following SBI (n= 4/group).

Neurologic outcome assessment with mGarcia score (B), beam balance score (C) and percentage of foot faults (D) at 24 hours following SBI showed that the beneficial effect of Mfsd2a CRISPR Act on neurologic functions was significantly diminished with the administration of Brusatol and ZnPP (n= 6/group).

Data are expressed as mean ± SD. ANOVA, Tukey. ** $p<0.001$ compared to Sham, * $p<0.05$ compared to Sham, # $p<0.05$ compared to SBI, && $p<0.001$ compared to SBI + Scramble CRISPR Act, & $p<0.05$ compared to SBI + Scramble CRISPR Act, $$ $p<0.001$ compared to SBI + Mfsd2a CRISPR Act (2 μg), $ $p<0.05$ compared to SBI + Mfsd2a CRISPR Act (2 μg).

SBI: Surgical brain injury

Table 1

The number and distribution of animals per experimental groups.

		Groups	Mortality (%)	Excluded (%)
Experiment 1	Time Course (Western Blot)	Sham (n= 4)	0	0
		SBI (6, 12, 24 and 72 hours) (n= 4/time point)	1	0
	Cellular Localization (Immunohistochemistry)	Sham (n= 1)	0	0
		SBI (n= 1)	0	0
Experiment 2	Verification of the Efficacy of CRISPR plasmids	Naive (n= 4)	0	0
		Mfsd2a CRISPR Act (2 μg, icv) (n= 4)	0	0
		Mfsd2a CRISPR KO (2 μg, icv) (n= 4)	0	0
	24-hour Outcome Study	Sham (n= 8)	0	0
		SBI (n= 8)	1	1
		SBI + Scramble CRISPR Act (icv) (n= 8)	0	0
		SBI + Mfsd2a CRISPR Act (2 μg, icv) (n= 8)	0	0
		SBI + Mfsd2a CRISPR Act (4 μg, icv) (n= 8)	0	0
		SBI + Scramble CRISPR KO (icv) (n= 6)	1	0
		SBI + Mfsd2a CRISPR KO (icv) (n= 6)	0	0
	Evans Blue Dye Extravasation	Sham (n= 6)	0	0
		SBI (n= 6)	2	0
		SBI + Scramble CRISPR Act (icv) (n= 6)	1	0
		SBI + Mfsd2a CRISPR Act (2 μg, icv) (n= 6)	1	0
Experiment 3	72-hour Outcome Study	Sham (n= 6)	0	0
		SBI (n= 6)	1	0
		SBI + Scramble CRISPR (icv) (n= 6)	1	0
		SBI + Mfsd2a CRISPR Act (2 μg, icv) (n= 6)	1	0
Experiment 4	Mechanism Study	Sham (n= 6)	0	0
		SBI (n= 6)	1	0
		SBI + Scramble CRISPR Act (icv) (n= 6)	1	0
		SBI + Mfsd2a CRISPR Act (2 μg, icv) (n= 6)	0	0
		SBI + Mfsd2a CRISPR Act (2 μg, icv) + Vehicle (10% DMSO, 4 μl) (n= 4)	0	0
		SBI + Mfsd2a CRISPR Act + Brusatol (1 mg/kg, icv) (n= 6)	1	0
		SBI + Mfsd2a CRISPR Act + ZnPP (3 mg/kg, iv) (n= 6)	0	0
	Co-immunoprecipitation	Sham (n= 4)	0	0
	SBI (n= 4)		0	0

		Groups	Mortality (%)	Excluded (%)	
	SBI + Scramble CRISPR Act (icv) (n= 4)		0	0	
	SBI + Mfsd2a CRISPR Act (2 μg, icv) (n= 4)		0	0	
	Total	204	190	13 (7.9)	1 (0.6)

Act: activation **CRISPR:** clustered regularly interspaced short palindromic repeat, **DMSO:** dimethyl sulfoxide, **icv:** intracerebroventricular, **iv:** intravenous, **KO:** knockout, **SBI:** Surgical brain injury